4A10 Flow instability

Fluid-structure interaction

CUED IIB Lecture notes

Shreyas Mandre

sdm63@cam.ac.uk

Last updated: Sun Mar 15 13:08:22 GMT 2026

Contents

Chapter 1

Introduction to stability

This chapter presents the concept of stability, especially linear stability. Much of the material is learned by the author through classical and authorative sources such as the books by Drazin and Reid[4] and Chandrasekhar[2]. The author especially recommends reading chapter 1 from the book by Chandrasekhar, which provides a detailed rationale behind the formulation of linear stability. It is this rationale that the present chapter attempts to reproduce in a form more accessible to beginners. While an elementary example is introduced in this chapter to facilitate discussion, knowledge of some flow instabilities such as Rayleigh-Plateau, Rayleigh-Taylor and thermal convection of Rayleigh-Benard instabilities will prove helpful.

1.1 Stability in terms of breaking symmetry

To understand the concept of symmetry breaking, consider a flat elastic plate, such as a postcard, subject to an oncoming flow aligned with the surface of the card. Such a situation is shown in fig. 1.1(a). The plate is cantilevered at the downstream end. Despite the configuration of this system being perfectly symmetric along the up-down axis, by virtue of interacting with the surrounding flow, the plate spontaneously bends along a direction perpendicular to the flow, as shown in fig. 1.1(b). This is an example of a system spontaneously breaking symmetry, in this case symmetry of reflection. The governing physics is symmetric under reflection about the dash-dotted line. This symmetry is also referred to as an invariance of the system to reflection, i.e. this system looks and behaves identically when reflected about the dash-dotted line. Yet the system spontaneously evolves towards a state that is not symmetric.

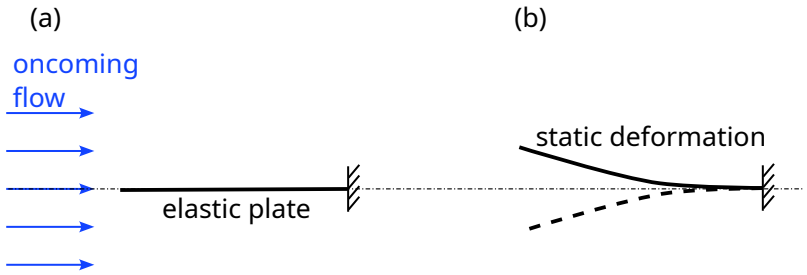

Figure 1.1: An illustration to explain breaking of symmetry. (a) A plate subject to oncoming flow and cantilevered at the downstream end. The flow is aligned with the surface of the plate. (b) The plate in (a) bending perpendicular to the flow.

Now consider a different kind of symmetry, that of time-translation invariance. For this symmetry, the example is that of blowing a raspberry. Relax your lip and slightly pucker them. Now gently blow through the lips taking care that you force the flow to be steady. With a little trial and error, you can get the lips to vibrate spontaneously. This is an example where the time-translation symmetry is broken. Here by time-translation symmetry, we mean the equivalence of every instance of time with every other. Because you are blowing steadily, the aerodynamic force on the lips is expected to be unchanging, or invariant, with time. The physical laws governing the motion of the lips are also invariant with time, i.e. they do not change with time. Yet, the lips spontaneously respond by executing time-dependent motion. In this manner, the invariance under time-translation is broken.

Spontaneous appearance of oscillations despite a steady forcing is a common occurence in nature and engineering. Examples include onset of phonation in our vocal cords, the production of sound in many musical

instruments such as organ pipes, flutes, clarinets, and the onset of oscillations that preceded disastrous collapse of the Tacoma Narrows Bridge in 1940.

Other examples of the symmetry are:

1. **Spatial translation symmetry**: A infinitely long thread of liquid exhibits spatial translation symmetry along its axis. Every location along its axis is equivalent to every other location. As you have learned, such a thread is susceptible to the Rayleigh-Plateau instability and breaks down into droplets. Different locations along the thread are no longer equivalent, because the droplets pinch off at some locations, while others form the centre of these droplets.

2. **Axisymmetry:** Wine forms tears when swirled in a glass. The shape of the glass is axisymmetric. When swirled, the wine coats the surface of the glass in nearly an axisymmetric manner. But as it falls down, the tear pattern that forms is not axisymmetric. This phenomenon is caused by gradients of surface tension through a mechanism known as the Marangoni effect.

Advanced tip. When a symmetry is broken by a system, it may be replaced by a lower symmetry. When axisymmetry is broken, for example in the aforementioned example of the tears of wine, the resulting pattern still obeys a discrete translation symmetry. In a perfectly controlled experiment, each wine tear will have a shape identical to all others.

1.2 The role of positive feedback in symmetry breaking

What causes symmetries in nature to be broken? The general explanation for broken symmetries is a positive feedback. Imagine that, for whatever reason, the system starts in a state that is not perfectly symmetric but there is a slight deviation from it. Perhaps the elastic plate is not perfectly aligned with the flow, or perhaps there is a slightly asymmetric gust of wind. Sources of perturbations are omnipresent, which cause the slightest of asymmetries to be introduced in the system. Such sources of asymmetry may be so weak that they are essentially invisible to us. However, the asymmetry causes the fluid dynamic force on the plate to also be slightly asymmetrical. If the nature of the dynamics is such that the resulting force on the system tends to amplify the asymmetry, then the asymmetry will naturally grow until it is noticeable and visible. Such is the nature of the positive feedback which breaks symmetry.

We will further elaborate on the various components of this mechanism using the following example, which is posed as an exercise for the reader.

Question 1.1. Aeroelastic divergence
Consider a simplified model of the flat plate in fig. 1.1, consisting of a rigid plate attached to a torsional spring via a hinge. A schematic is shown in fig. 1.2. The plate has length c along the flow, width w perpendicular to

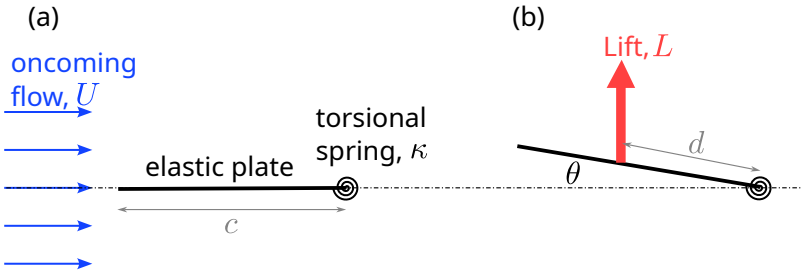

Figure 1.2: Schematic of a hinged plate (a) when aligned with the oncoming flow, and (b) when inclined to the flow an angle θ.

the plane of the page and the torsional spring constant is κ. The oncoming wind speed is U. When the plate makes an angle θ to the flow, the flow exerts a lift force $L = \frac{1}{2} C_L \rho U^2 cw \sin\theta$, where C_L is the lift coefficient, assumed constant, and ρ is the fluid density. The centre of lift is at a distance d from the hinge of the torsional spring. Determine the unbalanced torque on the plate when inclined at angle θ.

Answer 1.1. The restoring torque from torsional spring is $-\kappa\theta$ and the fluid dynamic torque is $\frac{1}{2}\rho U^2 cwd \sin\theta\cos\theta$ (the convention we use is that torques in the direction of increasing θ are positive). The net unbalanced torque, T, is

$$T = \frac{1}{2} C_L \rho U^2 cwd \sin\theta\cos\theta - \kappa\theta. \tag{1.1}$$

The torque tends to increase θ if $T > 0$, i.e. if

$$\frac{C_L \rho U^2 cwd}{2\kappa} > \frac{\theta}{\sin\theta\cos\theta}. \tag{1.2}$$

The left-hand side of eq. (1.2) depends only on the system parameters, while the right-hand side depends on the system configuration.

In question 1.1, the variable θ represents the degree of asymmetry. When the left-hand side of eq. (1.2), which depends only on the system parameters, exceeds the right-hand-side, which depends only on the system configuration, the feedback on the system asymmetry is positive, and the asymmetry will continue to grow spontaneously.

It is believed that Samuel Langley's attempts at flight were hindered by the problem of torsional aeroelastic divergence of wings[7]. The aircraft wing near the tips is susceptible to torsion along its span, which acts similar to the torsional spring in question 1.1. When the air flow speed exceeds a certain threshold, or when the torsional stiffness of the wing is small, in close analogy with the analysis in eq. (1.2), twisting of the wing increases the local angle of attack, which further increases the lift force causing the torsional deformation to grow. This is the mechanism of divergence. Torsional divergence is also a serious hindrance to the adoption of forward-swept wing design in subsonic and supersonic flight.

Section 1.2 presents an outline of the mechanism of symmetry breaking. How this type of mechanism can be analyzed systematically in general is presented in this chapter using the formalism of stability theory. The theory applies equally well to fluid dynamic stability as it does to fluid-structure instability, and indeed also extends to the realm beyond fluid or solid mechanics.

1.3 The state and state variables

From the physical system is carefully curated a set of quantities that are essential for the examination and analysis of the phenomenon under consideration. These quantities are termed as the state variables, which we will formally denote $\mathbf{x}$ for the remainder of this chapter. For the examination of a purely hydrodynamic instability, the fluid Eulerian velocity field is usually a part of the state variables. The shape of the interface between two fluids is also a part of the state variables when the motion of the interface is invoked, such as in the case of Rayleigh-Plateau and Rayleigh-Taylor instabilities. The state of temperature of the fluid could also be a part of the state variables for cases where the temperature influences the dynamics, such as in the case of Rayleigh-Benard convection or Marangoni convection.

The state variables are distinct from parameters in the sense that parameters are generally considered to be fixed in a given realization of the system, while the state variables are allowed to evolve with time t. Therefore, we tacitly consider $\mathbf{x}(t)$.

A specification of the state variables uniquely identifies the relevant portion of the state of the system necessary for understanding the mechanism of the instability. In the example of question 1.1, the state is defined by a single variable $\theta(t)$.

1.4 Dynamics governing the evolution of state

The state evolves in time according to the laws of nature, which govern the system under consideration. The governing evolution may depend on some system parameters, formally denoted as p. We formally write the governing physics limited to the phenomenon under consideration as

$$\frac{d\mathbf{x}}{dt} = \boldsymbol{\mathcal{F}}\left(\mathbf{x};\ p\right), \tag{1.3}$$

where $\boldsymbol{\mathcal{F}}$ is the function that determines the time-rate of change of the state. As stated earlier, note that p are treated as given and constant, so they do not evolve with time. If it is necessary for the system parameters to evolve with time, consider including them as part of the state.

For the example in question 1.1, let us further assume that the plate has negigible mass and its rotational motion about the hinge damps according to a damper with angular damping constant b. In other words, a torque $-bd\theta/dt$ about the hinge applies on the plate because of an angular damper. Then the motion of the plate is governed by the torque balance

$$b\frac{d\theta}{dt} = \frac{1}{2}C_L \rho U^2 cwd \sin\theta\cos\theta - \kappa\theta. \tag{1.4}$$

Here ρ, U, c, w, d, κ and b are system parameters.

Advanced tip. Enslaved variables: In some cases, the state variables are instantaneously related to others, and, therefore, it is either not possible or not the most convenient to write a rate-of-change function for them. Such variables are informally said to be enslaved to the remaining state variables. This usually happens when making an idealization or an approximation. A common example of such a case occurs when making the inviscid potential flow approximation for a fluid. In this case, the fluid velocity $\boldsymbol{u}$ is given in terms of a scalar velocity potential ϕ as $\boldsymbol{u} = \boldsymbol{\nabla}\phi$ and the potential itself satisfies $\nabla^2\phi = 0$. The rate-of-change of ϕ with time is available but only at the interface between fluids. This is, for example, the case for inviscid versions of Rayleigh-Plateau and Rayleigh-Taylor instabilities. Formally, in this case, we can consider the structure of the state variables and their evolution to be as follows. Consider the state to be made of two variables $\mathbf{x}$ and $\mathbf{y}$. A time-evolution equation is only available for $\mathbf{x}$ as

$$\frac{d\mathbf{x}}{dt} = \boldsymbol{\mathcal{F}}\left(\mathbf{x}, \mathbf{y};\ p\right). \tag{1.5}$$

And the instantaneous dependence between $\mathbf{x}$ and $\mathbf{y}$ is formally written as a relationship $\boldsymbol{\mathcal{G}}(\mathbf{x}, \mathbf{y}; p) = 0$. It is not possible or convenient to solve $\boldsymbol{\mathcal{G}}$ to write $\mathbf{y}$ in terms of $\mathbf{x}$, however, formally, a one-to-one relation between $\mathbf{x}$ and $\mathbf{y}$ exists and is depicted by $\boldsymbol{\mathcal{G}}$. While we will encounter such cases in practice (the inviscid Rayleigh-Plateau and Rayleigh-Taylor being two such cases), formally, we do not need to distinguish such cases from the formulation of eq. (1.3). It is so because, formally, $\mathbf{y}$ depends on $\mathbf{x}$ and thus $d\mathbf{x}/dt$ through $\boldsymbol{\mathcal{F}}$ can be determined using the knowledge of $\mathbf{x}$ alone.

In fact, the example in question 1.1 is a prime example of many of the approaches and strategies we employ in the interest of insight, including the topic of this advanced tip. In this example, on the one hand, we have allowed for the angle θ to change with time. This implies that the fluid flow around the plate is also dependent on time. And, therefore, the fluid pressure and the lift force on the plate also varies with time in a manner that depends on the flow. Hence, strictly speaking, we could have included the fluid velocity as a state variable and written the governing equations for the evolution of the flow – the Navier-Stokes equations. Instead, we tacitly assumed that the flow rapidly attains a steady state, in fact it does so instantaneously, for each angle θ. The lift force then only depends on θ, which we parameterize using the lift coefficient. The advantage of doing so is not only the simplicity it offers for the analysis but the opportunity it presents to arrive at the basic positive feedback mechanism, with explicit dependence on the parameters, albeit approximate.

Advanced tip. The symmetries of a system: The governing evolution equation eq. (1.3) must obey the the invariance with symmetries you have in mind for your system. For example, eq. (1.3) is time-translation invariant. This means defining a transformed time variable t' which is shifted relative to time t as $t' = t - \Delta t$ for an arbitrary constant Δt, and writing the governing evolution equation (1.3) in t' does not change the form of the function $\boldsymbol{\mathcal{F}}$.

The reflection symmetry of the example in question 1.1 means that the reflection transformation $\theta' = -\theta$, and eliminating θ in favour of θ' yields the same eq. (1.4) for the evolution of θ'.

Advanced readers will re-examine their past stability calculations and endeavour to determine all the symmetries of their governing evolution equations.

Advanced tip. The purpose of approximations: It is often mistakenly thought that the purpose of approximations is to enable an analytical solution. Such is not strictly the case. The purpose of approximations is to enable acquisition and development of insight into the physical mechanisms at play.

1.5 The steady state

Once the governing evolution equations for the state variable are established, we seek a steady state of these equations, especially one which obeys the symmetry of the system under investigation for being broken. Here are some examples:

1. For systems obeying time-translation symmetry, which is what we will consider exclusively in the rest of this chapter, we consider a state which is independent of time. This state is invariant under time translation transformation and thus obeys time-translation symmetry. For the case in question 1.1, we consider the possibility that the state θ is a constant in time.

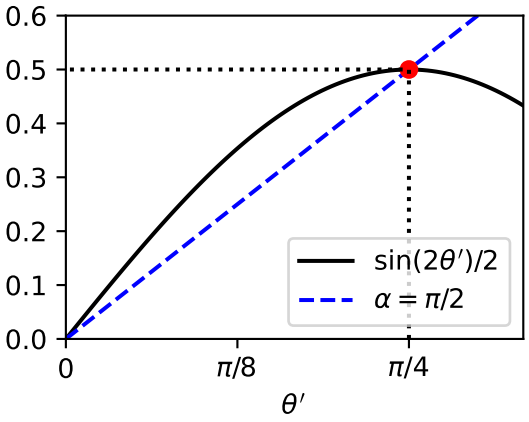

Figure 1.3: Comparison of two functions to understand the symmetry breaking transition of the hinged plate in question 1.1. The red dot shows the intersection of the two curves.

2. For systems obeying, spatial translation symmetry, such as in the case of Rayleigh-Plateau instability, one seeks a state that is constant along that spatial dimension. For Rayleigh-Plateau instability, the liquid thread radius is taken to be uniform along its axis to conform to the spatial translation symmetry along the axis. (Also note that for Rayleigh-Plateau, which also obeys time-translation symmetry, a state chosen is also steady.)

3. For systems with axisymmetry, an axisymmetric steady state is chosen.

For the case of question 1.1, which obeys a reflection symmetry and time-translation symmetry, we choose a steady reflection-symmetric state. The only such state is $\theta = \theta_0 = 0$. This state is identical to its reflection.

Advanced tip. Time-periodic systems and Floquet analysis: The interested advanced reader is referred to Floquet analysis for cases in which time-translational symmetry does not apply. In such cases, one does not (or rather can not) seek a steady state in this step.

Formally, let us denote this state as $\mathbf{x}_0$. This state satisfies

$$\boldsymbol{\mathcal{F}}\left(\mathbf{x}_0;\ p\right) = 0. \tag{1.6}$$

That $\theta = 0$ obeys eq. (1.4) is readily verified.

1.6 Perturbation of the steady state

Our goal now is to determine the fate of any perturbation away from the steady state we determined in section 1.5. For this purpose, we define the perturbation variable $\mathbf{x}'$ as

$$\mathbf{x} = \mathbf{x}_0 + \mathbf{x}', \tag{1.7}$$

and eliminate $\mathbf{x}$ in favour of $\mathbf{x}'$. Substituting in eq. (1.3) yields the evolution equation that governs the fate of the perturbation.

$$\frac{d\mathbf{x}'}{dt} = \boldsymbol{\mathcal{F}}\left(\mathbf{x}_0 + \mathbf{x}';\ p\right), \tag{1.8}$$

where we have used the steady nature of $\mathbf{x}_0$ so that $d\mathbf{x}_0/dt = 0$.

For our example in question 1.1, the perturbation is $\theta = \theta_0 + \theta' = 0 + \theta' = \theta'$. Therefore, θ' satisfies

$$b\frac{d\theta'}{dt} = \frac{1}{2}C_L\rho U^2 cwd\sin\theta'\cos\theta' - \kappa\theta'. \tag{1.9}$$

In rare cases, such as for eq. (1.9), it is possible to examine the evolution equation for the perturbation and deduce the fate of the perturbation – see the Advanced tip below.

Advanced tip. Without loss of generality, let us exploit the reflection symmetry and only consider the case θ' positive. The analysis for negative θ' may be obtained by reflecting the analysis for positive θ'. Whether the perturbation angle grows or decays depends on the dimensionless parameter $\alpha = \dfrac{C_L \rho U^2 cwd}{2\kappa}$ and the angle θ' itself. The perturbation angle grows when right-hand side of eq. (1.9) is positive, i.e when $\dfrac{\sin(2\theta')}{2} > \dfrac{\theta'}{\alpha}$, and decays otherwise. It is readily deduced that if $\alpha < 1$, then the torsional spring restoring torque always exceeds the aerodynamic torque. For $\alpha > 1$, the aerodynamic torque exceeds the torsional spring torque only if θ' is within a range $(0, \theta_{eq})$, where $\theta_{eq} \neq 0$ satisfies $\dfrac{\sin(2\theta_{eq})}{2} = \dfrac{\theta_{eq}}{\alpha}$. An example of such a case is shown in fig. 1.3 for $\alpha = \pi/2$, for which case $\theta_{eq} = \pi/4$. In this range, θ' grows. For $\theta' > \theta_{eq}$, the torsional restoring torque is greater and causes θ' to decay.

Thus, we can conclude the following. If the initial perturbation is exactly zero, i.e. the environment is devoid of sources of perturbation, the plate will stay perfectly aligned with the flow. However, this is unlikely because sources of perturbations in the environment are omnipresent and will likely perturb the plate to a non-zero angle. If $\alpha < 1$, this perturbation will decay and the plate will not be visibly perturbed from $\theta = 0$. However, if α exceeds unity, then the plate angle will not return to zero. If the random perturbation kicks the plate to a positive (negative) angle, then the aerodynamic torque will cause the plate angle to rise (fall) all the way to θ_{eq} ($-\theta_{eq}$). If the perturbation is too strong and pushes the plate angle beyond α_{eq}, then the angle will fall back to a value around θ_{eq}. This will be the fate of the plate. The symmetry of the plate angle will be spontaneously broken because of the random perturbations always present in every environment.

However, in the general case, especially when the governing evolution is not as simple and clean as in question 1.1, this type of analysis is not feasible. There are techniques called "Energy stability", which can sometimes provide useful information about the stability characteristics. These are outside the scope of this text.

1.7 Linearization

While in the general case, the inference about the stability, positive feedback and symmetry breaking may not be deduced from the equivalent of eq. (1.8), much can be gained by considering a perturbation of infinitesimal size. The rationale for considering infinitesimal perturbations is that it provides a so-called mathematically sufficient condition for instability and symmetry breaking. In the best and most careful experiments, sources of noise and perturbations cannot be completely eliminated and thus are unavoidable. Eliminating perturbations becomes more and more difficult as the perturbation size becomes smaller and smaller. Thus, a system free of small perturbations is an idealization that cannot be practically realized. At the very least, thermal fluctuations are always present. If the natural evolution of the system is such that the tiniest of the perturbations grow in magnitude, then that state is impossible to maintain. Thus, if we can determine that infinitesimal perturbations necessarily grow, then we can safely conclude that such a steady state cannot be maintained. In this manner, we can deduce a sufficient condition for instability and symmetry breaking.

The other reason for considering infinitesimal perturbations is that the arsenal of mathematical techniques that can be deployed for analysis expands. Powerful techniques based on linear algebra can be brought to bear upon the resulting analysis. We will examine these techniques in the next section.

In this section, let us make pursue the consequences of assuming that the perturbations are infinitesimal, i.e. the magnitude of $\mathbf{x}'$ approaches zero. In this case, the right-hand side of eq. (1.8) may be simplified using a Taylor expansion as

$$\boldsymbol{\mathcal{F}}\left(\mathbf{x}_0 + \mathbf{x}';\ p\right) = \boldsymbol{\mathcal{F}}(\mathbf{x}_0;\ p) + \frac{\delta \boldsymbol{\mathcal{F}}}{\delta \mathbf{x}}\left(\mathbf{x}_0;\ p\right)\mathbf{x}' + \text{higher order terms.} \tag{1.10}$$

Here, by construction of the steady state $\mathbf{x}_0$, $\boldsymbol{\mathcal{F}}(\mathbf{x}_0;\ p) = 0$, and therefore the first nontrivial term that remains on the right-hand side is the linear term. In the limit as the magnitude of $\mathbf{x}'$ approaches zero, the higher order terms limit to zero, and are formally neglected.

Advanced tip. The astute reader may have recognized that the existence of the Taylor expansion relies on the function $\boldsymbol{\mathcal{F}}$ being sufficiently smooth at $\mathbf{x} = \mathbf{x}_0$. It is indeed true that such conditions of differentiability must be satisfied by $\boldsymbol{\mathcal{F}}$. In practice, finding examples that do not satisfy the requisite differentiability criteria do exist, require a suitable modification to the above simplification, and lead to interesting results in their

own right. For example, see John Norton's Dome paradox, popularized on YouTube by Jade Tan-Holmes. Suffice to say, a vast number of cases commonly encountered do subject themselves to the simple Taylor expansion presented in eq. (1.10), so we proceed without concerning ourself with the degenerate cases.

With the Taylor expansion of $\boldsymbol{\mathcal{F}}$, the evolution of the infinitesimal perturbation obeys the linear equation

$$\frac{d\mathbf{x}'}{dt} = \boldsymbol{\mathcal{L}}\left(\mathbf{x}_0;\ p\right)\mathbf{x}', \quad \text{where} \quad \boldsymbol{\mathcal{L}}\left(\mathbf{x}_0;\ p\right) = \frac{\delta \boldsymbol{\mathcal{F}}}{\delta \mathbf{x}}\left(\mathbf{x}_0;\ p\right) \tag{1.11}$$

is formally the linear operator that acts on the infinitesimal perturbation.

For the case in question 1.1, the perturbation evolution eq. (1.9) simplifies upon assuming and infinitesimal perturbation θ' to

$$b\frac{d\theta'}{dt} = \left(\frac{1}{2}C_L\rho U^2 cwd - \kappa\right)\theta'. \tag{1.12}$$

Here we have used $\sin\theta' \approx \theta'$ and $\cos\theta' \approx 1$, and deduced that the higher order terms in this approximation do not enter the linear expression. We shall use this equation in further analysis.

1.8 A word about non-dimensionalization

This stage is ripe for examining the dimensions of the perturbation variables, the terms in their evolution equation eq. (1.11), and the dependence on the set of parameters p. It is often insightful to use physical intuition to identify scales of mass, length, time and any other relevant dimensions using the parameters p, and construct any dimensionless variables that govern the linear system.

In the example presented in question 1.1, the plate perturbation relaxes back to equilibrium on a time scale b/κ in the absence of flow. We can choose this scale to non-dimensionalize time as $\tilde{t} = t\kappa/b$, and eliminate t in favour of $\tilde{t}$. In doing so, we also introduce $\alpha = \dfrac{C_L\rho U^2 cwd}{2\kappa}$ as the only dimensionless parameter. The perturbation angle now satisfies the dimensionless governing equation

$$\frac{d\theta'}{d\tilde{t}} = (\alpha - 1)\,\theta'. \tag{1.13}$$

Note that this step is optional, but if taken, the convenience of the analysis, the quality of result, and the level of insight obtained generally improves greatly.

1.9 Normal modes and exponential growth

As mentioned before, the linear nature of eq. (1.11) allows us to unleash the full potential of linear algebra to bear upon this topic. The first property to exploit is based on the definition of linearity itself. If $\mathbf{x}'_1(t)$, $\mathbf{x}'_2(t)$, $\ldots$, $\mathbf{x}'_n(t)$ all satisfy eq. (1.11), then so does their linear combination

$$\mathbf{x}'(t) = c_1\mathbf{x}'_1(t) + c_2\mathbf{x}'_2(t) + \cdots + c_n\mathbf{x}'_n(t), \tag{1.14}$$

where c_1, c_2, $\ldots$, and c_n are arbitrary constants.

Secondly, we can exploit the time-translation invariance of eq. (1.11) and assert an exponential growth for the perturbation in time. Mathematically,

$$\mathbf{x}'(t) = \hat{\mathbf{x}}e^{st}, \tag{1.15}$$

where $\hat{\mathbf{x}}$ is a constant vector of the same dimensions as $\mathbf{x}'$, and s is the so-called growth rate associated with $\hat{\mathbf{x}}$. Substituting in eq. (1.11) reveals the relation between $\hat{\mathbf{x}}$ and s as

$$s\hat{\mathbf{x}} = \boldsymbol{\mathcal{L}}\hat{\mathbf{x}}, \tag{1.16}$$

which is an eigenvalue equation for s. According to eq. (1.16), s must be an eigenvalue of $\boldsymbol{\mathcal{L}}$ and $\hat{\mathbf{x}}$ the corresponding eigenvector (or eigenfunction, as the case may be). Note that, here we suppress explicitly writing the arguments of $\boldsymbol{\mathcal{L}}(\mathbf{x}_0;\ p)$. Supposing $\boldsymbol{\mathcal{L}}$ has a complete spectrum $\{\hat{\mathbf{x}}_1, \hat{\mathbf{x}}_2, \ldots, \hat{\mathbf{x}}_n\}$, i.e. a set of eigenvectors that spans the linear space defined by $\mathbf{x}'$, with corresponding eigenvalues $s_1, s_2, \ldots, s_n$, respectively, arranged in descending order of their real parts (i.e. $\Re(s_1) \geq \Re(s_2) \geq \cdots \geq \Re(s_n)$) the general solution for eq. (1.11) may be written as

$$\mathbf{x}'(t) = c_1\hat{\mathbf{x}}_1e^{s_1t} + c_2\hat{\mathbf{x}}_2e^{s_2t} + \cdots + c_n\hat{\mathbf{x}}_ne^{s_nt}. \tag{1.17}$$

Here by completeness, we mean that $\hat{\mathbf{x}}_1$, $\hat{\mathbf{x}}_2$, ..., $\hat{\mathbf{x}}_n$ form a basis for the linear space of perturbations $\mathbf{x}'$. This is the formal presentation of the method for solving a linear first order differential equation of the form of eq. (1.11). Here the constants $c_1, c_2, \ldots, c_n$ are to be determined by the initial condition given as $\mathbf{x}'(t=0) = \mathbf{x}'_i$, so that

$$\mathbf{x}'_i = c_1\hat{\mathbf{x}}_1 + c_2\hat{\mathbf{x}}_2 + \cdots + c_n\hat{\mathbf{x}}_n, \tag{1.18}$$

which yields unique values for c_1, c_2, ..., c_n owing to the completeness of the spectrum.

Advanced tip. Time-translation invariance and exponential growth: The dependence between time-translational invariance for linear systems and exponential growth is deep and can be understood at an intuitive level in the following sense. Time-translation invariance implies the equivalence between any two instances of time, and linearity implies growth of the perturbation proportional to its current amplitude. Thus, the two together imply that if a perturbation amplifies at a certain rate at time t_1 when its amplitude is a_1, then at a later time t_2 when its amplitude has become a_2, the growth rate ought to be proportional to a_2. This implies that its amplification rate remains the same at time t_2 as it is at time t_1. The function of time that captures these two properties is the exponential. The amplification rate is embodied by the growth rate s.

In the case of question 1.1, eq. (1.13) is a scalar equation, i.e. the linear space of perturbation θ' is one-dimensional. The solution to eq. (1.13) is

$$\theta'(\tilde{t}) = \theta'_i e^{s\tilde{t}}, \quad \text{where} \quad s = (\alpha - 1)\,. \tag{1.19}$$

1.10 Sufficient condition for instability

At this stage, we interpret the result comprising of eqs. (1.17) and (1.18) in terms of the sufficient condition for instability. We invoked earlier our inability to control the source of perturbations as the inspiration for undertaking this analysis. We now state that relation between the external source of perturbation and the mathematically formulation as follows. The external perturbation source forces an initial condition $\mathbf{x}'_i$, whose subsequent evolution is determined by the preceding analysis. While the source of perturbation is omnipresent, we only need to concern ourselves with the response of our system at a time to one perturbation that causes the initial condition $\mathbf{x}'_i$. It is so because if this one perturbation grows and disrupts the state of the systems, then it is unlikely that the other perturbations conspire in a way to exactly negate the disruption. Underlying this assumption is the impossibility of eliminating infinitesimal perturbations, and thus $\mathbf{x}'_i$ can not be zero.

Similarly, we have no control over the shape of the perturbation. This lack of control implies an absence of knowledge of the exact shape of $\mathbf{x}'_i$, and a tacit treatment of the initial condition as a random variable drawn from a suitable distribution. While this should take us into the realm of probability and stochastic differential equations, hydrodynamic stability avoids following such a route. Instead, the theory concludes that the randomness of $\mathbf{x}'_i$ and the decomposition eq. (1.18) implies that none of the constants c_1, c_2, ..., c_n may be assumed to vanish. This, in turn implies in the light of eq. (1.17), that whether the perturbation grows or decays depends solely on the growth rates s_1, s_2,...,s_n, especially their real parts, and in this way, circumvents the uncertainty of the perturbation shape.

Since we arranged the growth rates in descending order, we infer that all infinitesimal perturbations decay if $\Re(s_1) < 0$. Such modes are called *linearly stable* and when all the modes are stable, the system is said to be *linearly stable*. This by itself is not a strong inference because it only applies to infinitesimal perturbations. It is silent about perturbations of a finite amplitude. However, if $\Re(s_1) > 0$, then at least one mode must grow despite being infinitesimal in amplitude. The exponentially growth of this mode prevents the system from approaching the steady state $\mathbf{x}_0$, and the steady state $\mathbf{x}_0$ becomes impossible to maintain. Such a mode $\hat{\mathbf{x}}_1$ is called *linearly unstable*. Furthermore, if $\hat{\mathbf{x}}_1$ is the only unstable eigenvector, i.e. one with an eigenvalue such that $\Re(s_1) > 0$, then we also expect the shape of this mode to be observed in the system. When an unstable mode is present, the system on the whole is considered to be *linearly unstable*.

As the parameters p are changed, the modes of the system may transition from being stable to unstable. The threshold of stability is determined by the condition that the eigenvalue of $\boldsymbol{\mathcal{L}}$ with the largest real part is either zero or purely imaginary, i.e. $\Re(s) = 0$. Such modes are called *neutral modes*, which neither grow nor decay, and the parameter values at which these modes appear is the *threshold of linear instability* or the *critical condition for the onset of linear instability*. Much of linear stability analysis concerns itself with classifying parameter space into linearly stable and unstable regions.

For the example in question 1.1, there is only one growth rate, $s = \alpha - 1$. This growth rate is negative when $\alpha < 1$ and positive when $\alpha > 1$. Thus linear instability ensues when $\alpha > 1$, which is the critical condition for the onset of instability. In dimensional terms, the parameter measures the relative strength of the aerodynamic force

to the elastic force. When the destabilizing aerodynamic force exceeds the stabilizing elastic force, instability ensues. The critical speed, called the divergence speed, for this structure can be determined from the threshold condition to be

$$U = \sqrt{\frac{2\kappa}{C_L \rho c d w}}. \tag{1.20}$$

1.11 Conclusion

The purpose of the analysis is to gain insight. This motivates making simplifying assumptions so that we can understand the influence of and interaction between various physical effects. While it is difficult to ascertain the fate of arbitrary perturbations made to a system, the framework of linear algebra facilitates the analysis of infinitesimal perturbations. We exploit this to the fullest in linear stability analysis and arrive at a sufficient condition for the disruption of a steady state.

The preceding formalism applies with little modification to cases where the degrees of freedom are finite. In systems that contain an infinite number of degrees of freedom, such as for a continuum fluid, and especially one which is infinite in spatial extent, some of these considerations need to be revisited, the precise meaning of spectrum, eigenvectors and stability need to be analyzed separately and carefully on a case-by-case basis. Some of the modern developments in stability theory, including spatial versus temporal stability, non-normality of modes, resolvent analysis, transient growth of perturbations have arisen from such considerations.

We conclude by noting that linear stability theory is silent about ultimate the fate of the unstable perturbation mode. In some instances, a weakly nonlinear theory may be constructed to determine this fate, but such a treatment is outside the scope of this chapter.

Chapter 2

Simple models for structures

Description of both fluid flows and elastic structures require infinite degrees of freedom along each of the three spatial dimensions. Doing so may be necessary in some circumstances, but hinders uncovering of basic stability principles. Where possible, it is prudent to judiciously retain only a few degrees of freedom as part of the stability analysis. In this chapter, we will revise some simple models to represent structures.

In many cases, the instability arises from the fluid flow forcing the structure to excite one or few of the natural modes of oscillation of the structure. Under such a circumstance, it is prudent to represent the state of the structure by a few state variables that are excited during the oscillations of those modes. The simplest of such variables is an amplitude of the natural mode, which behaves like a (possibly damped) harmonic oscillator, with equivalent lumped parameters. In this chapter, a generic fluid dynamic force on these degrees of freedom is assumed.

Making this approximation is not entirely without merit, as will be shown in some of the cases below using the method of projection. In doing so, we will practice the method of linearization and the calculation of normal modes, which will also prepare us for such analysis in case of coupled fluid-structure interaction. In addition, we will also consider some structural stability problems in their own right, using the method of linear stability analysis outlined in chapter 1.

2.1 Lumped mass-spring-damper

Sometimes, a structure may be approximated simply as a rigid point mass m attached to a spring with stiffness k and a damper with coefficient b, as shown in fig. 2.1. A generic fluid dynamic force on the mass is denoted f.

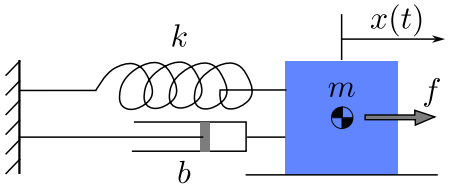

Figure 2.1: Schematic of a mass-spring-damper lumped mass system.

The displacement $x(t)$ is the sole state variable describing this system. It obeys

$$m\frac{\mathrm{d}^2x}{\mathrm{d}t^2} + b\frac{\mathrm{d}x}{\mathrm{d}t} + kx = f. \tag{2.1}$$

Note that this equation is already linear, so a linearization of this equation around any steady state will not alter it. Also, note that an energy equation can be constructed by multiplying this equation by $\mathrm{d}x/\mathrm{d}t$ as

$$\frac{\mathrm{d}}{\mathrm{d}t}\left[\frac{1}{2}m\left(\frac{\mathrm{d}x}{\mathrm{d}t}\right)^2 + \frac{1}{2}kx^2\right] = -b\left(\frac{\mathrm{d}x}{\mathrm{d}t}\right)^2 + f\frac{\mathrm{d}x}{\mathrm{d}t}. \tag{2.2}$$

The rate of energy removed by the damper is $b(\mathrm{d}x/\mathrm{d}t)^2$ and the work done by the fluid is $f\mathrm{d}x/\mathrm{d}t$.

Question 2.1. Determine the motion of the mass in the absence of the fluid dynamic force and starting from an arbitrary initial condition.

Answer 2.1. The natural frequence of a free undamped harmonic oscillator (i.e. $f = 0$ and $b = 0$) is given by $\omega_0 = \sqrt{k/m}$. Based on this, the underdamped motion of a free damped oscillator (i.e. $f = 0$ but $b \neq 0$) may be written in terms of the dimensionless variables $\omega_0 t = \tilde{t}$ and $\beta = b/2\sqrt{km}$. The equation of motion for the mass then becomes

$$\frac{\mathrm{d}^2 x}{\mathrm{d}\tilde{t}^2} + 2\beta \frac{\mathrm{d}x}{\mathrm{d}\tilde{t}} + x = 0. \tag{2.3}$$

Since this equation is already linear, we can follow the prescription of section 1.9 and try a solution of the form $x(t) \propto e^{s\tilde{t}}$, to get the following eigenvalue equation for s,

$$s^2 + 2\beta s + 1 = 0, \qquad \text{which has roots} \qquad s = -\beta + i\sqrt{1-\beta^2}. \tag{2.4}$$

(Note that the nature of the eigenvalue equation is quadratic in this case.) This yields the motion to be

$$x(t) = e^{-\beta\tilde{t}} \left(a_1 \cos\omega\tilde{t} + a_2 \sin\omega\tilde{t} \right), \quad \text{where} \quad \omega^2 = 1 - \beta^2. \tag{2.5}$$

Here the condition for the motion being underdamped is $\beta < 1$.

Question 2.2. Possibly nonlinear spring: Suppose that the spring is not a Hookean or linear spring, and the restoring force it produces is $-kx - qx^3$. Write the equation governing the state variable x. Also derive any equation for the energy of the system.

Answer 2.2. The restoring force appears in the governing equations as

$$m\frac{\mathrm{d}^2 x}{\mathrm{d}t^2} + b\frac{\mathrm{d}x}{\mathrm{d}t} + kx + qx^3 = f. \tag{2.6}$$

The energy equation for this case is

$$\frac{\mathrm{d}}{\mathrm{d}t}\left[\frac{1}{2}m\left(\frac{\mathrm{d}x}{\mathrm{d}t}\right)^2 + \frac{1}{2}kx^2 + \frac{1}{4}qx^4 \right] = -b\left(\frac{\mathrm{d}x}{\mathrm{d}t}\right)^2 + f\frac{\mathrm{d}x}{\mathrm{d}t}. \tag{2.7}$$

The spring is strain-stiffening if $q > 0$ and strain-softening if $q < 0$.

The spring in the damped mass-spring system can be nonlinear, such as in question 2.2, and so can be the damper.

Question 2.3. The nonlinear mass-spring system is subject to a constant external fluid dynamic force f. Determine the steady state of the system in response to this force. Linearly perturb this state to determine the equation governing the evolution of the perturbation. Determine whether the perturbation would grow or decay, especially for the strain-softening case $q < 0$.

Answer 2.3. The new steady state displacement of the mass, x_0, balances the spring restoring force with the applied fluid dynamic force.

$$kx_0 + qx_0^3 = f. \tag{2.8}$$

A closed form expression for x_0 in terms of k, q and f may not be possible. We perturb this state as $x = x_0 + x'$, to yield the equation for the perturbation as

$$m\frac{\mathrm{d}^2 x'}{\mathrm{d}t^2} + b\frac{\mathrm{d}x'}{\mathrm{d}t} + kx' + q(x_0 + x')^3 - qx_0^3 = f - kx_0 - qx_0^3 = 0, \tag{2.9}$$

where we have used eq. (2.8) to simplify the right-hand side of eq. (2.9). Further, taking the perturbation x' to be infinitesimal, the nonlinear term of eq. (2.9) may be linearized as $q(x_0 + x')^3 - qx_0^3 \approx 3qx_0^2 x'$. Thus,

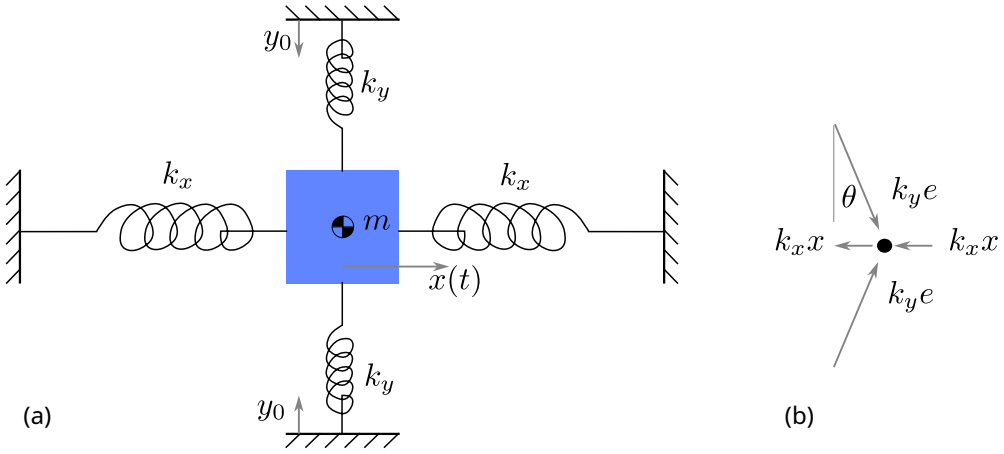

Figure 2.2: Schematic for the model of buckling. (a) A mass suspended by four springs in equilibrium. (n) Free body diagram for the mass when it is displaced along the x direction.

the linear equation governing the perturbation becomes

$$m\frac{\mathrm{d}^2x'}{\mathrm{d}t^2} + b\frac{\mathrm{d}x'}{\mathrm{d}t} + (k + 3qx_0^2)x' = 0. \tag{2.10}$$

Equation (2.10) is a linear damped mass-spring equation in its own right, where the equivalent spring stiffness of $k + 3qx_0^2$. If the nonlinear spring is strain-softening, $q < 0$, the equivalent spring is softer. If $k + 3qx_0^2$ becomes negative, the spring does not produce a restoring force, but instead provides a positive feedback for the perturbation to grow. The threshold condition is $k + 3qx_0^2 = 0$, which combined with eq. (2.8), yields the criteria on the critical f to be $f_{\text{critical}} = \dfrac{2}{3\sqrt{3}}\dfrac{k^{3/2}}{(-q)^{1/2}}$.

Note that the nonlinear spring force produces a restoring force for any displacement less than $x_0 = \sqrt{-k/q}$, but stably holding the extension at any value greater than $\sqrt{-k/3q} = x_0/\sqrt{3}$ is impossible due to sensitivity to perturbations.

Determining the scales for x and t, as well as the dimensionless parameters from eq. (2.6) is a worthy exercise in dimensional analysis. Performing this analysis and following it with the linear stability analysis in dimensionless terms is left for the astute reader.

Question 2.4. Consider a mass m suspended symmetrically between four springs. Two are along the x axis of stiffness k_x and two are along the y axis of stiffness k_y. The springs along y have a rest length of L_y. The mass is at the origin when all the springs are at their equilibrium length. The springs along y are then compressed by a length y_0. A schematic of this setup is shown in fig. 2.2(a). Examine the stability of the mass under translation along x.

Answer 2.4. Here x, the displacement of the mass m is the state variable. Free body diagram of the mass m in the displaced state is shown in fig. 2.2(b). The two springs along x exert a restoring force of strength $k_x x$. The extension and orientation of the springs along y must also be determined to examine their influence on the mass. These springs make an angle $\theta = \tan^{-1}\left(\dfrac{x}{L_y - y_0}\right)$. The compression of the spring is $e = L_y - \sqrt{(L_y - y_0)^2 + x^2}$, and the force along the length of the spring is $k_y e$. The equation governing the state, therefore, is

$$m\frac{\mathrm{d}^2x}{\mathrm{d}t^2} = -2k_x x + 2k_y e\sin\theta. \tag{2.11}$$

Since the equilibrium to investigate is $x = 0$, the perturbation $x' = x$ obeys the same equation as x. When the perturbation is infinitesimal in size, we have

$$\sin\theta \approx \theta \approx \frac{x}{L_y - y_0}, \quad \text{and} \quad e \approx y_0 \tag{2.12}$$

The linear equation governing the infinitesimal perturbation is

$$m\frac{\mathrm{d}^2x'}{\mathrm{d}t^2} = 2\left(-k_x + \frac{k_y y_0}{L_y - y_0}\right)x'. \tag{2.13}$$

An examination of the dimensions suggest defining a dimensionless time as $\tilde{t} = t\sqrt{k_y/m}$ and the follwing two parameters $\tilde{e} = y_0/L$ and $\tilde{k} = \dfrac{k_x}{k_y}$. The variable x' may be non-dimensionalized by any length. The dimensionless equation governing the perturbation is

$$\frac{\mathrm{d}^2x'}{\mathrm{d}\tilde{t}^2} = 2\left(-\tilde{k} + \frac{\tilde{e}}{1-\tilde{e}}\right)x'. \tag{2.14}$$

The right hand side is equivalent to a modified spring with dimensionless stiffness $\tilde{k} - \tilde{e}/(1-\tilde{e})$, which forebodes instability if it becomes negative. Therefore, the criteria for the onset on instability is $\tilde{e} > \dfrac{\tilde{k}}{1+\tilde{k}}$.

The mechanism is evident from fig. 2.2(b). This is a simplified model of buckling of a structure.

2.2 Pitch and heave

The next simplest structure has two degrees of freedom. An example is depicted schematically in fig. 2.3, where they are the rotational degree called pitch, θ, and the translational degree of freedom called heave, h. While fig. 2.3 shows a symmetric airfoil, the object could be of arbitrary shape. It has mass m and moment of inertia about the centre of mass $I = mR_g^2$, where R_g is the radius of gyration. The object is supported at the centre of support, which is a distance x_s away from the centre of mass, as shown in the figure. A translational spring with linear stiffness k, and a torsional spring with rotational stiffness κ' support the object at the centre of support. And the object also experiences an aerodynamic force of lift, L, in the direction of heave at the centre of pressure, which is a distance x_a from the centre of mass. We ignore any damping that may be present in this structure for this analysis.

The state variables h and θ describe the dynamical state of the object. The evolution of the state is governed by force and torque balance around the centre of mass and satisfies the following equations

$$m\ddot{h} + kh + kx_s\sin\theta = L, \tag{2.15}$$

$$I\ddot{\theta} + kx_s h\cos\theta + \kappa'\theta + kx_s^2\sin\theta\cos\theta = Lx_a\cos\theta, \tag{2.16}$$

where the double-dot decoration above h and θ means the second derivative with time t. For what follows, we will ignore the external force of lift, i.e. take $L = 0$, and examine the structural dynamics. For this purpose, we determine the steady state to be $h = 0$ and $\theta = 0$. Perturbation about the steady state are made as $h = 0 + h'$ and $\theta = 0 + \theta'$. Assuming the perturbations to be small (i.e. infinitesimal), they satisfy

$$m\ddot{h'} + kh' + kx_s\theta' = 0, \tag{2.17a}$$

$$I\ddot{\theta'} + kx_s h' + \kappa\theta' = 0, \tag{2.17b}$$

where $\kappa = \kappa' + kx_s^2$. These equations may also be expressed in terms of the state vector $\mathbf{x} = [h, \theta]^T$ as

$$\boldsymbol{M}\ddot{\mathbf{x}} + \boldsymbol{K}\mathbf{x} = 0, \qquad \boldsymbol{M} = \begin{bmatrix} m & 0 \\ 0 & I \end{bmatrix}, \qquad \boldsymbol{K} = \begin{bmatrix} k & kx_s \\ kx_s & \kappa \end{bmatrix} \tag{2.18}$$

where $\boldsymbol{M}$ is the mass matrix and $\boldsymbol{K}$ is the stiffness matrix. Note that both are symmetric and positive definite.

An equation for energy can be constructed by multiplying eq. (2.17a) with $\dot{h}' = \mathrm{d}h'/\mathrm{d}t$ and eq. (2.17b) with $\dot{\theta}' = \mathrm{d}\theta'/\mathrm{d}t$ and adding them to yield

$$\frac{\mathrm{d}}{\mathrm{d}t}\left[\frac{1}{2}m\dot{h'}^2 + \frac{1}{2}I\dot{\theta'}^2 + \frac{1}{2}kh'^2 + kx_s h'\theta' + \frac{1}{2}\kappa\theta'^2\right] = 0, \tag{2.19}$$

or in matrix notation, where $\dot{\mathbf{x}} = \mathrm{d}\mathbf{x}/\mathrm{d}t$,

$$\frac{\mathrm{d}}{\mathrm{d}t}\left[\frac{1}{2}\dot{\mathbf{x}}^T\boldsymbol{M}\dot{\mathbf{x}} + \frac{1}{2}\mathbf{x}^T\boldsymbol{K}\mathbf{x}\right] = 0. \tag{2.20}$$

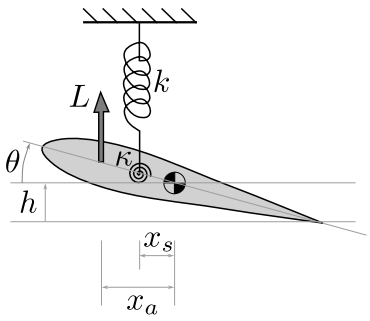

Figure 2.3: Schematic showing a structure with two degrees of freedom – pitch θ and heave h.

The energy equation guides the rescaling towards a dimensionless formulation with the rescaling

$$t = \tilde{t}\sqrt{\frac{m}{k}}, \quad h' = R_g\tilde{h}, \quad \theta' = \tilde{\theta}, \quad \delta = \frac{2x_s}{R_g}, \quad \text{and} \quad \omega_a^2 = \frac{\kappa}{kR_g^2}. \tag{2.21}$$

The dimensionless equations governing the perturbations are

$$\frac{\mathrm{d}^2\tilde{h}}{\mathrm{d}\tilde{t}^2} + \tilde{h} + \frac{\delta}{2}\tilde{\theta} = 0, \tag{2.22}$$

$$\frac{\mathrm{d}^2\tilde{\theta}}{\mathrm{d}\tilde{t}^2} + \frac{\delta}{2}\tilde{h} + \omega_a^2\tilde{\theta} = 0. \tag{2.23}$$

The parameter δ serves as the coupling between the two degrees of freedom. If $\delta = 0$, pitch and heave are uncoupled and each have a natural frequency of ω_a and 1, respectively. Because energy neither grows nor decays in this system, we expect pure oscillations for the two degrees of freedom, even when they are coupled. Since these equations are linear, we may seek exponentially growing solutions $e^{i\omega\tilde{t}}$, so that $s = i\omega$ satisfies

$$\begin{bmatrix} 1 & \delta/2 \\ \delta/2 & \omega_a^2 \end{bmatrix} \begin{bmatrix} \tilde{h} \\ \tilde{\theta} \end{bmatrix} = \omega^2 \begin{bmatrix} \tilde{h} \\ \tilde{\theta} \end{bmatrix}. \tag{2.24}$$

Solving the eigenvalue equation yields for the two values of ω^2

$$\frac{(1-\omega^2)}{\delta/2} = \frac{\delta/2}{(\omega_a^2 - \omega^2)} \qquad \Longrightarrow \qquad \omega_{1,2}^2 = \frac{1 + \omega_a^2 \pm \sqrt{\delta^2 + (1-\omega_a^2)^2}}{2}. \tag{2.25}$$

The first property we note is that ω^2 is real, so the growth rate is purely imaginary and thus there is neither growth nor decay of the perturbations. When $\delta = 0$, the frequencies agree with our expectation for the uncoupled degrees of freedom. A real physical system will show decay of these perturbations owing to some damping.

The corresponding eigenvectors are

$$\hat{\mathbf{x}}_{1,2} = \begin{bmatrix} \tilde{h} \\ \tilde{\theta} \end{bmatrix} = \begin{bmatrix} \delta/2 \\ \omega_{1,2}^2 - 1 \end{bmatrix} = c \begin{bmatrix} \omega_{1,2}^2 - \omega_a^2 \\ \delta/2 \end{bmatrix}, \tag{2.26}$$

where c is a constant, which ensures that the lengths of the two forms of the eigenvector are equal to each other. It can be readily seen from eq. (2.26) that when $\delta = 0$, the eigenvectors have either the h component or θ, but not both, thus verifying that in this case the two modes are indeed decoupled. In this case, naturally the dot product between the two independent eigenvectors is zero, so they are orthogonal. The orthogonality between the two eigenvectors for the case $\delta \neq 0$ can be easily verified using the forms in eq. (2.26) and the property that $\omega_1^2 + \omega_2^2 = 1 + \omega_a^2$. This nifty property is left for the reader to discover.

2.3 A general structure with a finite number of degrees of freedom

In general, an abstract structure with a finite degrees of freedom may be represented using the state variable vector $\mathbf{x}$, where the vector has as many components as the degrees of freedom. The state vector can obey an equations for its evolution written as eq. (1.3) from section 1.4. Let us consider the case where the undeformed state is given by $\mathbf{x} = 0$ is the steady state, where there are no external forces, and all displacements and internal forces vanish. However, in the absence of damping, the dynamics must conserve energy, and therefore, the

following form for the evolution emerges for the perturbation $\mathbf{x}'$ when linearized about the undeformed steady state.

$$\boldsymbol{M}\frac{\mathrm{d}^2\mathbf{x}'}{\mathrm{d}t^2} + \boldsymbol{K}\mathbf{x}' = 0, \tag{2.27}$$

where $\boldsymbol{M}$ is the mass matrix and $\boldsymbol{K}$ the stiffness matrix. Both $\boldsymbol{K}$ and $\boldsymbol{M}$ are symmetric and positive-definite matrices. These matrices in general may not be diagonal or sparse. The system conserves the energy E defined as

$$E = \frac{1}{2}\dot{\mathbf{x}'}^T\boldsymbol{M}\dot{\mathbf{x}'} + \frac{1}{2}\mathbf{x}'^T\boldsymbol{K}\mathbf{x}'. \tag{2.28}$$

For this reason, any perturbation made around the steady state must oscillate, say with frequency ω. The frequency satisfies the eigenvalue equation

$$\boldsymbol{K}\hat{\mathbf{x}} = \omega^2\boldsymbol{M}\hat{\mathbf{x}}, \tag{2.29}$$

where the state is assumed to evolve as $\mathbf{x}' = \hat{\mathbf{x}}e^{i\omega t}$. Solution of this equation yields both the many natural frequencies ω_i and the corresponcing mode shapes $\hat{\mathbf{x}}_i$, for $i = 1, 2, \ldots, n$, where n is the number of degrees of freedom. Because of the symmetry and positive-definiteness of $\boldsymbol{K}$ and $\boldsymbol{M}$, we are guaranteed that the frequencies are real and that the various modes are mutually orthogonal, i.e.

$$\hat{\mathbf{x}}_j^T\boldsymbol{M}\hat{\mathbf{x}}_i = 0 \quad \text{when} \quad j \neq i. \tag{2.30}$$

Using the properties of $\hat{\mathbf{x}}_i$ and ω_i, we may construct the general evolution of the perturbation in the presence of an external forcing, say from the surrounding fluid. If the infinitesimal forcing on the structure is written as $\mathbf{f}$, it responds according to

$$\boldsymbol{M}\frac{\mathrm{d}^2\mathbf{x}'}{\mathrm{d}t^2} + \boldsymbol{K}\mathbf{x}' = \mathbf{f}. \tag{2.31}$$

It is possible to look for a solution to eq. (2.31) of the form

$$\mathbf{x}'(t) = a_1(t)\hat{\mathbf{x}}_1 + a_2(t)\hat{\mathbf{x}}_2 + \cdots + a_n(t)\hat{\mathbf{x}}_n, \tag{2.32}$$

where $a_1(t)$, $a_2(t)$, $\ldots$, $a_n(t)$ are amplitudes of the various modes, which are to be determined. (Here we assume that the mode shapes $\hat{\mathbf{x}}_1$, $\hat{\mathbf{x}}_2$, $\ldots$, $\hat{\mathbf{x}}_n$ have been precomputed.) Substituting eq. (2.32) into eq. (2.31), then yields

$$\sum_{i=1}^{n}\left(\ddot{a}_i + \omega_i^2 a_i\right)\boldsymbol{M}\hat{\mathbf{x}}_i = \mathbf{f}, \tag{2.33}$$

where we have used eq. (2.29) and the double-dot decoration denoted second derivative in t. Now, exploit orthogonality of the eigenvectors from eq. (2.30), and take a dot product with one of the eigenvectors $\hat{\mathbf{x}}_j$. Noting that all the terms in the sum vanish, except for the $i = j$, then yields the equation for the amplitude $a_i(t)$ as

$$\ddot{a}_i + \omega_i^2 a_i = \frac{\hat{\mathbf{x}}_i^T\mathbf{f}}{\hat{\mathbf{x}}_i^T\boldsymbol{M}\hat{\mathbf{x}}_i}. \tag{2.34}$$

In this manner, the response of a structure to an external forcing can be determined by projection on the natural modes of oscillation of the structure.

2.4 A stretched string or a one-dimensional membrane

A string or a wire that is stretched along it length (say, in the direction of the x-axis) presents a simple model for a continuum elastic structure. The wire length is L, tension in the wire is T and it has a mass μ per unit length, as shown in fig. 2.4. The point on this string at the coordinate x displaces in a direction perpendicular to the length (the Y-direction) by a distance $y(x,t)$. If an external force f per unit length is applied to the string along the y-direction, the displatement obeys

$$\mu\frac{\partial^2 y}{\partial t^2} = T\frac{\partial^2 y}{\partial x^2} + f. \tag{2.35}$$

The displacement of the string is zero at the two ends $x = 0$ and $x = L$.

Figure 2.4 also shows a membrane stretched along x with tension T per unit length. The tension perpendicular to plane of the page (i.e. along the z direction) does not enter the formulation because $\dfrac{\partial}{\partial z} = 0$. In this case, μ is the mass of the membrane per unit area, and f is the external force per unit area perpendicular to the

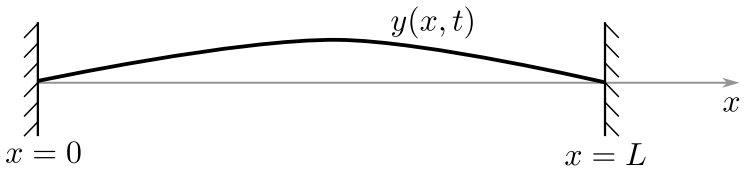

Figure 2.4: A string or a membrane stretched between $x = 0$ and $x = L$, which has a transverse displacement $y(x, t)$.

membrane. The membrane displacement $y(x, t)$ is also governed by eq. (2.35). Because of the analogy between the one-dimensional membrane and a stretched string, we will only consider the string from now on.

The stretched string satisfies the energy equations

$$\frac{\partial}{\partial t}\int_0^L \left[\frac{\mu}{2}\left(\frac{\partial y}{\partial t}\right)^2 + \frac{T}{2}\left(\frac{\partial y}{\partial x}\right)^2\right] \mathrm{d}x = \int_0^L f\frac{\partial y}{\partial t}\,\mathrm{d}x. \tag{2.36}$$

Here the integral proportional to μ is the kinetic energy, the one proportional to T is the elastic potential energy, and the right-hand side is the work done by the external force. For the stretched membrane a trivial integral along z may also be included.

Let us first determine the natural modes of vibrations of the string (or the membrane, as the case may be). For the natural modes, we set $f = 0$. The equilibrium shape of the string in this case is $y = 0$. Perturbing the displacement from the steady state as $y = 0 + y'$ yields the equation for the perturbation

$$\mu\frac{\partial^2 y'}{\partial t^2} = T\frac{\partial^2 y'}{\partial x^2}. \tag{2.37}$$

This equation is already linear so no further approximation for an infinitesimal perturbation needs to be made.

To make the formulation dimensionless, we define $\tilde{t} = \dfrac{t}{L}\sqrt{\dfrac{T}{\mu}}$ and $\tilde{x} = x/L$, so eq. (2.37) becomes

$$\frac{\partial^2 y'}{\partial \tilde{t}^2} = \frac{\partial^2 y'}{\partial \tilde{x}^2}, \qquad \text{for} \quad 0 < \tilde{x} < 1, \tag{2.38}$$

and $y'(\tilde{x} = 0, \tilde{t}) = y'(\tilde{x} = 1, \tilde{t}) = 0$.

When $f = 0$, energy is conserved, so we expect perturbations to neither grow nor decay. Hence we seek a solution to eq. (2.38) of the form $y' = \hat{y}(\tilde{x})e^{i\omega\tilde{t}}$. The mode shape $\hat{y}(\tilde{x})$ satisfies

$$\frac{\mathrm{d}^2\hat{y}}{\mathrm{d}\tilde{x}^2} + \omega^2\hat{y} = 0 \tag{2.39}$$

with $\hat{y} = 0$ at $\tilde{x} = 0$ and 1. A non-trivial solution only exists if $\omega = \omega_n = n\pi$ for $n = 1, 2, \ldots$, in which case the mode shape is

$$\hat{y}_n(\tilde{x}) = \sin(n\pi\tilde{x}). \tag{2.40}$$

The mode shapes satisfy the orthogonality condition

$$\int_0^1 \hat{y}_n(\tilde{x})\hat{y}_m(\tilde{x})\,\mathrm{d}\tilde{x} = 0, \qquad \text{if} \quad m \neq n, \tag{2.41}$$

which can be easily verified. (Note that the notion of dot products is replaced by integrals in this case.)

If an external force acts on the string, we can determine the response of the string in the following manner. First, we transform eq. (2.35) to a dimensionless form by using $\tilde{f} = fL^2/T$ to yield

$$\frac{\partial^2 y'}{\partial \tilde{t}^2} = \frac{\partial^2 y'}{\partial \tilde{x}^2} = \tilde{f}, \tag{2.42}$$

Let us write the perturbation as a linear combination of the modes as

$$y'(x, t) = \sum_{n=0}^{\infty} a_n(t)\hat{y}_n(\tilde{x}). \tag{2.43}$$

Substituting eq. (2.43) in eq. (2.42), with the intention of determining how the amplitudes $a_n(t)$ respond to the forcing $\tilde{f}$, yields

$$\sum_{n=1}^{\infty} \left(\ddot{a}_n + \omega_n^2 a_n\right) \hat{y}_n(\tilde{x}) = \tilde{f}(\tilde{x}, \tilde{t}), \tag{2.44}$$

where, as before, the double-dot decoration denotes second derivative with $\tilde{t}$. We use orthogonality to decouple the evolution of distinct modes. For doing so, we multiply with $\hat{y}_m(\tilde{x})$ and integrate along $\tilde{x}$ as

$$\int_0^1 \hat{y}_m(\tilde{x}) \left[\sum_{n=1}^{\infty} \left(\ddot{a}_n + \omega_n^2 a_n\right) \hat{y}_n(\tilde{x})\right] \, \mathrm{d}\tilde{x} = \int_0^1 \hat{y}_m(\tilde{x}) \tilde{f}(\tilde{x}, \tilde{t}) \, \mathrm{d}\tilde{x}. \tag{2.45}$$

The orthogonality condition from eq. (2.41) then facilitates the simplification

$$\ddot{a}_m + \omega_m^2 a_m = \frac{\int_0^1 \hat{y}_m(\tilde{x}) \tilde{f}(\tilde{x}, \tilde{t}) \, \mathrm{d}\tilde{x}}{\int_0^1 \hat{y}_m(\tilde{x})^2 \, \mathrm{d}\tilde{x}}. \tag{2.46}$$

2.5 Euler beam

The stretched string serves as an example that applies the general formalism of normal modes to determine the response of a continuum structure to external forcing. To test their understanding, the reader is invited to apply the formalism to the example of an Euler beam. The state of the beam is again described by the variable $y(x, t)$, which satisfies the governing equation

$$\mu \frac{\partial^2 y}{\partial t^2} = -B \frac{\partial^4 y}{\partial x^4} + T \frac{\partial^2 y}{\partial x^2} + f. \tag{2.47}$$

Here μ, T, and f are the same as before, and B is the bending stiffness or bending rigidity of the beam cross section. In what follows, we will take the tension T to be zero. This equations must be supplemented with two boundary conditions at each end, which are of the form

1. A given linear combination of displacement and shear force is specified,

$$ay - Bb \frac{\partial^3 y}{\partial x^3} = r_1(t), \tag{2.48}$$

and

2. A given linear combination of the slope and the bending moment is specified,

$$c \frac{\partial y}{\partial x} + Bd \frac{\partial^2 y}{\partial x^2} = r_2(t), \tag{2.49}$$

where a, b, c, d, r_1 and r_2 are specified constants. Without loss of generality, b and d may be taken to be unity so long as they are non-zero. These boundary conditions may be interpreted as the ends of the beam being supported by linear and torsional springs of stiffness a and c, respectively, and an external force (r_1) or torque (r_2) being applied there.

Question 2.5. Derive the principle of conservation of energy for the Euler beam that satisfies eqs. (2.47) to (2.49).

Answer 2.5. Multiply eq. (2.47) by $\partial y/\partial t$ and integrate in x from 0 to L, with a few judicious integrations by parts and application of the boundary conditions, to get

$$\frac{1}{2} \frac{\partial}{\partial t} \left\{ \int_0^L \left[\mu \left(\frac{\partial y}{\partial t} \right)^2 + B \left(\frac{\partial^2 y}{\partial x^2} \right)^2 \right] \, \mathrm{d}x + \left[\frac{a}{b} y^2 + \frac{c}{d} \left(\frac{\partial y}{\partial x} \right)^2 \right]_0^L \right\} = \int_0^L f \, \frac{\partial y}{\partial t} \, \mathrm{d}x + \left[\frac{r_1}{b} \frac{\partial y}{\partial t} + \frac{r_2}{d} \frac{\partial^2 y}{\partial x \partial t} \right]_0^L. \tag{2.50}$$

The term proportional to μ is the kinetic energy of the beam, the term proportional to B is the bending energy (which is proportional to square of curvature), the terms proportional to a and c are the energies stored in the linear and torsional springs at the end, the term proportional to f on the right hand side is the work done by the distributed external force, and the terms proportional to r_1 and r_2 are the works done by the external boundary forces and torques. Here we have tacitly assumed that b and d are positive, so they can be taken to be unity. The diligent reader is left the task of deriving the version of this equation when b and d are zero.

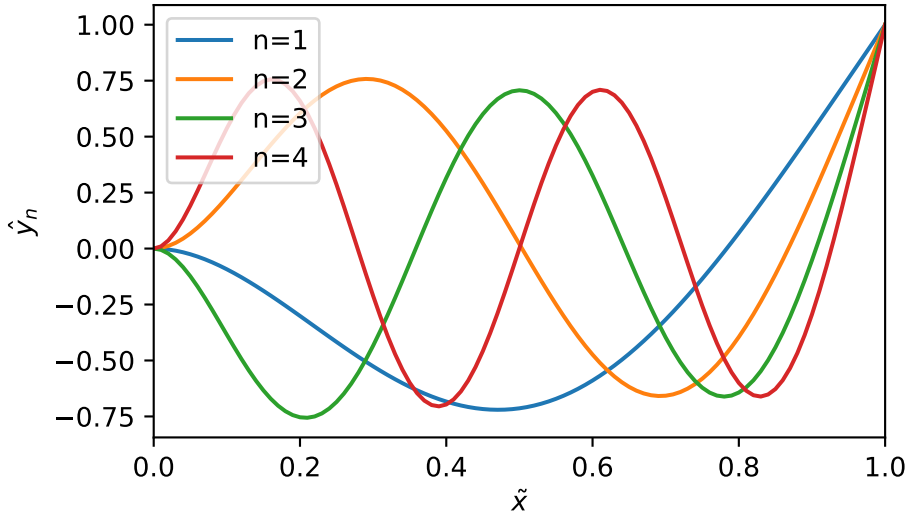

Figure 2.5: Shapes of the first few modes of oscillations of the Euler beam.

Question 2.6. Determine the frequency and shapes of the natural modes of oscillations of a cantilevered beam. (For a cantilevered beam, at one end the displacement and angle are zero, while at the other end the moment and shear force are zero.)

Answer 2.6. We use the non-dimensionalization:

$$\tilde{t} = t\sqrt{\frac{\mu L^4}{B}}, \qquad \tilde{x} = \frac{x}{L}. \tag{2.51}$$

It is left as an exercise to the reader to derive the eigenvalue equation for the natural dimensionless frequency ω and the mode shape $\hat{y}(\tilde{x})$, which is

$$\frac{\partial^4 \hat{y}}{\partial \tilde{x}^4} = \omega^2 \hat{y}, \tag{2.52}$$

with $\hat{y} = \mathrm{d}\hat{y}/\mathrm{d}\tilde{x} = 0$ at $\tilde{x} = 0$ and $\mathrm{d}^2\hat{y}/\mathrm{d}\tilde{x}^2 = \mathrm{d}^3\hat{y}/\mathrm{d}\tilde{x}^3 = 0$ at $\tilde{x} = 1$. Let $k = \omega^{1/2}$, i.e. the positive square root of ω, because it is convenient to write the expressions in terms of k. The general solution of eq. (2.52) is

$$\hat{y}(\tilde{x}) = a\sinh k\tilde{x} + b\sin k\tilde{x} + c\cosh k\tilde{x} + d\cos k\tilde{x}, \tag{2.53}$$

where a, b, c and d are constants of integration. Some of these constants are determined by the boundary conditions. For instance, the conditions at $\tilde{x} = 0$ imply $b = -a$ and $d = -c$, so they may be eliminated. The boundary conditions at $\tilde{x} = 1$ then require

$$a(\sinh k + \sin k) + c(\cosh k + \cos k) = 0, \tag{2.54a}$$
$$a(\cosh k + \cos k) + c(\sinh k - \sin k) = 0. \tag{2.54b}$$

The only solution for general k is $a = c = 0$, but that is the trivial solution to eq. (2.52). A non-trivial solution exists only when the two equations in eq. (2.54) are identical. The condition for a non-trivial solution to exist is

$$\cosh k \cos k = -1, \tag{2.55}$$

which is satisfied by a countably infinite values of k, say $k_1, k_2, \ldots$. The first few values are: $k_1 = 4.69409113$, $k_2 = 7.8547$, $k_3 = 10.9955$, $k_4 = 14.1372$. For large n, the value of k_n may be approximated to be

$$k_n = \left(n + \frac{1}{2}\right)\pi + \frac{(-1)^n}{\cosh\left(n + \frac{1}{2}\right)\pi}$$

This formula can be seen to be acurate for $n = 2$ upto four decimal places, and gets more and more accurate for larger n. The accuracy of this formula can be determined by evaluating the respective k_n and

substituting the result in eq. (2.55). The dimensional natural frequency of oscillations may now be written as

$$\Omega_n = k_m^2 \sqrt{\frac{B}{\mu L^4}}. \tag{2.56}$$

The mode shape is given by

$$\hat{y}_n(\tilde{x}) = C\left(\frac{\sinh k_n\tilde{x} - \sin k_n\tilde{x}}{\sinh k_n + \sin k_n} - \frac{\cosh k_n\tilde{x} - \cos k_n\tilde{x}}{\cosh k_n + \cos k_n}\right), \tag{2.57}$$

where C is an arbitrary constant. These mode shapes are visualized in fig. 2.5.

It is left as an exercise to the reader to either verify or prove the the othogonality condition eq. (2.41), which these modes obey. The author does not recommend actually multiplying $\hat{y}_m$ with $\hat{y}_n$ and integrating to prove the orthogonality condition.

2.6 Conclusion

In this chapter, we considered simple models for some structures and analyzed their behaviors in terms of perturbations about the steady state. In cases where we expected harmonic oscillations, we were able to apply the formalism of linear theory to determine the mode shape and natural frequency by assuming a time dependence of $e^{i\omega t}$, for some real ω. In cases where we expected an instability, we were also able to apply linear theory to determine the exponential growth of the unstable perturbations.

In this process, we found that while the deformation of the structure itself may be most complicated, it may be decomposed into mode shapes, which exhibit a simple harmonic behaviour for their amplitude. We also saw the method of projection, which exploits orthogonality of modes, to decouple the influence of a general external forcing on individual modes.

We also constructed the energy conservation principle for the structures we considered, including the influence of the external forcing on the rate of change of energy. The energy of a perturbation is a good indicator of its growth or decay, and therefore the derivation of an energy equation is instrumental in stability analyses.

The matter in this chapter is only but an introduction to the otherwise rich subject of structures and elasticity, and especially to the topic of simplified descriptions of them. Prime topic in this subject, which we omitted, is the theory of rods, shells and plates, which presents a one- and two-dimensional approximation to three-dimensional objects which are thin along the remaining dimension(s). Furthermore, structural instabilities are a formidable topic in their own right, without the need for the complicated coupling with the fluid flow.

We conclude with the following question on the buckling of elastic beams.

Question 2.7. Consider an Euler beam governed by eq. (2.47), which is under compression, so $T < 0$, say $T = -F$. Assume simply pinned boundary conditions so that $b = r_1 = c = r_2 = 0$, and without loss of generality $a = d = 1$. There are no external forces on the beam, so $f = 0$. The beam buckles when the compressive force F exceeds a threshold. Use the formulation of linear stability analysis to determine this threshold.

Answer 2.7. $\left(F_{\text{critical}} = \dfrac{B\pi^2}{L^2}\right)$.

The answer is provided, but the process of arriving at it is entrusted to the keen reader so that they can sharpen their abilities.

Chapter 3

Simple models for fluids

The fluid flow around objects or through conduits is commonly characterized by a velocity U. This could be the speed of wind or water far upstream, called the freestream speed. Or this could be the average speed of the fluid through enclosed channels, such as pipes and conduits. Without loss of generality, such a speed is a system parameter, which influences the fluid dynamic force on the structure. In addition to the fluid speed, the other relevant properties of the fluid are its density ρ and viscosity μ.

The sensible reader has immediately realized that the parameters ρ, μ and U, which characterize the fluid flow, cannot be combined into any dimensionless form by themselves. If the flow is to change character, such as a transition from a stable state to an unstable state, say by itself or when coupled with a structure, then the critical parameter must be dimensionless. The parameter U feels essential (although we may get a chance to examine a situation which is not chacterized by a speed.) Therefore, U must be combined with ρ and/or μ, along with some more parameters we have not yet recognized. At the very least, the fluid dynamic force on the structure must have the appropriate dimensions and depend on the relevant quanitites in a physically meaningful way. Gaining insight into this dependence is the objective of this chapter.

3.1 Parametrization in the viscous and inviscid limit

The state of the fluid in general is expressed by the Eulerian velocity field $\boldsymbol{u}(\boldsymbol{x}, t)$. The state evolution is governed by the Navier-Stokes equations (here we will assume incompressible flow, $\boldsymbol{\nabla} \cdot \boldsymbol{u} = 0$)

$$\rho \left[\frac{\partial \boldsymbol{u}}{\partial t} + (\boldsymbol{u} \cdot \boldsymbol{\nabla}) \boldsymbol{u} \right] + \boldsymbol{\nabla} p = \boldsymbol{f} + \mu \nabla^2 \boldsymbol{u}, \tag{3.1}$$

where p is the fluid pressure, which enforces the incompressibility, and $\boldsymbol{f}$ is the external volumetric force. The term on the left-hand side proportional to ρ represents the inertia of the fluid and the one on the right-hand size proportional to μ represents the viscosity. A general analytical solution of eq. (3.1) in combination with the required boundary conditions of interest has not been possible and is, therefore, outside the scope of this module. This equation may be solved computationally, and this is a very popular endeavour, one which we will not pursue in this module in the interest of insight.

The rescaling $\boldsymbol{u} = U\tilde{\boldsymbol{u}}$ to make $\boldsymbol{u}$ dimensionless must necessarily be accompanied by the rescaling of t and $\boldsymbol{x}$, but what would determine the scales for these variables?

> **Advanced tip.** There is a length scale $\ell = \mu/(\rho U)$ that can be constructed from the fluid parameters. Similarly there is also a time scale $\tau = \mu/(\rho U^2)$. However, the relevant question is whether the flow speed varies by the magnitude U over points separated by these length and time scales. It is generally found that these scales are associated with turbulence, which is a purely fluid dynamical phenomenon, once the scale for the flow speed is given some thought and possibly replaced by an apropriate value. Therefore, ℓ and τ do not seem necessarily connected with the interaction of the fluid with the structure.

Generally, the boundary of the fluid and/or the region it occupies introduces scales for length L and time T. These could be the diameter of the sphere or cylinder immersed in the flow, or the chord of an airfoil, or the diameter of a pipe through which the fluid flows. When they are used for non-dimensionalization as $\boldsymbol{x} = L\tilde{\boldsymbol{x}}$ and $t = T\tilde{t}$, two dimensionless numbers appear in the rescaled eq. (3.1).

$$\frac{L}{UT} \frac{\partial \tilde{\boldsymbol{u}}}{\partial \tilde{t}} + (\tilde{\boldsymbol{u}} \cdot \tilde{\boldsymbol{\nabla}}) \tilde{\boldsymbol{u}} + \tilde{\boldsymbol{\nabla}} \tilde{p} = \tilde{\boldsymbol{f}} + \mathrm{Re}^{-1} \tilde{\nabla}^2 \tilde{\boldsymbol{u}}, \tag{3.2}$$

where $p = \rho U^2 \tilde{p}$, $\tilde{\boldsymbol{f}} = \boldsymbol{f} L/\rho U^2$, and $\mathrm{Re} = \rho UL/\mu$ is the Reynolds number, named after Osborne Reynolds. Of course, if the boundaries move too slowly, so that $T \gg L/U$, then the response of the flow to that motion may be considered quasisteady and the time-rate-of-change term $\partial \tilde{\boldsymbol{u}}/\partial \tilde{t}$ may be neglected.

The Reynolds number charcterizes the relative strength of inertia to viscosity in a given situation.

3.1.1 Low Reynolds number flow

When the Reynolds number is small, viscosity dominates over inertia. The inertial term may be neglected to yield the celebrated Stokes equations, named after George Gabriel Stokes, as

$$-\boldsymbol{\nabla} p + \mu \nabla^2 \boldsymbol{u} = \boldsymbol{f}. \tag{3.3}$$

(In the boundary of the fluid moves sufficiently fast $T \ll \rho L^2/\mu$, then the time-derivative of $\boldsymbol{u}$ may not be ignored.) This equation is combined with boundary conditions about the motion of the boundary, where the fluid velocity is specified. The Stokes equations are linear in the velocity and pressure, and, therefore, linear in the relation between the velocity of the boundary and the force on the boundary. In addition, time does not enter the formulation of Stokes flow except through the motion of the boundaries. The flow adjusts instantaneously to the motion of the boundary. (This principle was illustrated by Taylor in 1967[9] in what has now become an iconic video.) The linearity and kinematic reversibility of eq. (3.3) helps immensely in determining the flow and, more importantly, characterizing the forces exerted by such a fluid on strutures. The essence of this argument may be found in the notes by Taylor[8] in this document.

For a general object of length scale L immersed in the fluid, moving with a steady speed U and rotating with angular speed Ω at low Reynolds numbers, the drag F_D, lift F_L and torque Q exerted by the fluid may be written as

$$F_D = C_{t,D} \mu U L + C_{r,D} \mu \Omega L^2, \tag{3.4a}$$

$$F_L = C_{t,L} \mu U L + C_{r,L} \mu \Omega L^2, \quad \text{and} \tag{3.4b}$$

$$Q = C_{t,Q} \mu U L^2 + C_{r,Q} \mu \Omega L^3, \tag{3.4c}$$

where $C_{t,D}$, $C_{r,D}$, $C_{t,L}$, $C_{r,L}$, $C_{t,Q}$ and $C_{r,Q}$ are dimensionless coefficients, which depend on the shape of the body but not its size. For example, for a translating and rotating sphere, $C_{t,D} = 3\pi$, $C_{r,D} = C_{t,L} = C_{r,L} = C_{t,Q} = 0$ and $C_{r,Q} = \pi$, where L is the diameter of the sphere. For details, the reader is referred to the authoritative account by Happel and Brenner[6] on this topic.

3.1.2 High Reynolds number flow

When the Reynolds number is large, inertia dominates over viscosity everywhere in the fluid, except in a thin boundary layer. In this case, the response of the fluid to the presence and motion of the solid structure is much more complicated compared to the case of low Reynolds number. Progress is possible in some cases, such as for streamlined wings based on the application of thin airfoil theory. In other cases, much insight can still be derived from a suitable parameterization of the fluid dynamic forces.

3.1.3 Steady lift on thin airfoils

Two-dimensional potential flow theory applied to thin airfoil explains the flow around real streamlined airfoil cross section for small angles of attack when the flow remains attached. The theory predicts that a thin streamlined cross section of chord c making an angle of attack α with the oncoming flow experiences a lift force F_L per unit length perpendicular to the cross section given by

$$F_L = \frac{1}{2} \rho U^2 c \, C_L(\alpha, \mathrm{Re}), \qquad \text{where} \qquad C_L(\alpha, \mathrm{Re}) \approx 2\pi\alpha, \tag{3.5}$$

where C_L is called the lift coefficient. The theory by itself predicts no drag in the inviscid limit. However, when combined with boundary layer theory, the drag per unit length F_D is parameterized as

$$F_D = \frac{1}{2} \rho U^2 c \, C_D, \tag{3.6}$$

where C_D is called the drag coefficient. Multiple physical effects contribute to the drag, and an approximate parameterization of $C_D(\alpha, \mathrm{Re})$ may be possible in many cases. We will take C_D to be given in this module.

This theory only applies in the steady or quasi-steady case, where the time-scale over which the angle of attack changes T is large compared to the aerodynamic time scale c/U, i.e. $UT/c \gg 1$. When $UT/c \sim O(1)$ or $UT/c \ll 1$, an unsteady version of the potential flow theory called Wagner's theory applies. The details of this theory are outside the scope of this module.

3.1.4 Steady bluff body drag

Bluff bodies have shapes for which flows with high Reynolds number do not remain attached to the surface of the body but instead separate. This process of separation causes vorticity to be shed from the boundary layer to the region behind the body and a wake to develop. Due to the separation, the flow deviates significantly from potential flow. The flow in the wake is not strictly steady because turbulence usually develops in this region. (We will discuss the origin of this unsteadiness later in this module when we discuss vortex-induced vibrations.) The flow in the wake may still be considered statistically steady, i.e. steady on average on a time-scale much longer than those of turbulent eddies. Based on this, a parameterization on the average steady drag, $\overline{F}_D$, may be written as

$$\overline{F}_D = \frac{1}{2}\rho U^2 A\, \overline{C}_D, \tag{3.7}$$

where A is the frontal area presented by the body to the flow and $\overline{C}_D$ is the average dimensionless drag coefficient. Equation (3.7) is a parameterization of the drag, which is based on an incomplete understanding of the physics, and, therefore, $\overline{C}_D$ is strictly an unknown function of Re, which is measured empirically. An insightful manner of proceeding pretends $\overline{C}_D$ to be known, and proceeds to draw conclusions, just to realize that many of the conclusions do not depend sensitively on the precise value of $\overline{C}_D$.

The assumption of statistical steadiness requires a small discussion. On the one hand, the flow changes slowly enough that the parameter UT/L is large, where L is the representative length of the bluff body. On the other hand, the unsteadiness in the wake caused by turbulence is assumed to be fast and statistically stationary so that it may be averaged out. (For phenomena such as vortex-induced vibrations, this type of separation of scales is violated, so watch out for this counterexample.)

In the same spirit as eq. (3.7), an asymmetric bluff body in the flow may also experience a lift force. This lift may be parameterized as

$$\overline{F}_L = \frac{1}{2}\rho U^2 A\, \overline{C}_L, \tag{3.8}$$

where $\overline{C}_L$ is the average dimensionless lift coefficient.

3.2 Simplified versions of Navier-Stokes

In some cases, it is possible to simplify from the three-dimensional nature of Navier-Stokes equations to a one-dimensional. We discuss some such cases in this section.

3.2.1 Force on an unsteady curved fluid-carrying conduit

Consider a flexible conduit, with centreline described by a given unsteady curve $\boldsymbol{X}(s,t)$, where s is the arc-length along the centreline, carrying a fluid with constant density ρ. The shape and area of the conduit cross-section does not vary along its length, and the cross section is assumed to be much smaller than the typical radius of curvature. The fluid is approximated to be inviscid, and to flow with speed U with a uniform profile across the

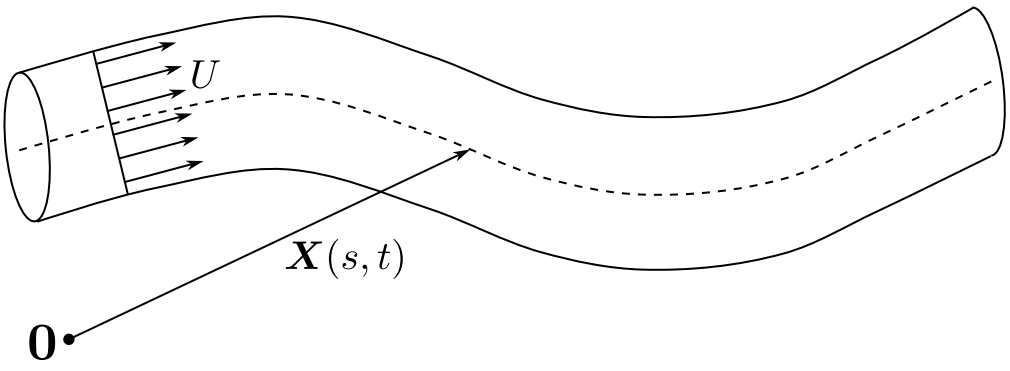

Figure 3.1: A flexible conduit with centreline following the curve $\boldsymbol{X}(s,t)$ conveying a fluid with speed U uniformly across its cross section.

cross section of the conduit. A schematic of such a conduit is shown in fig. 3.1. The objective is to determine the force exerted by the fluid on the conduit.

The fluid velocity relative to the conduit is everywhere tangent to the curve centreline $\hat{\boldsymbol{t}} = \partial \boldsymbol{X}/\partial s$, and is therefore given by

$$\boldsymbol{u} = \frac{\partial \boldsymbol{X}}{\partial t} + U\frac{\partial \boldsymbol{X}}{\partial s} = \left(\frac{\partial}{\partial t} + U\frac{\partial}{\partial s}\right)\boldsymbol{X}. \tag{3.9}$$

The acceleration of the fluid is the material derivative of the velocity

$$\boldsymbol{a} = \left(\frac{\partial}{\partial t} + U\frac{\partial}{\partial s}\right)\boldsymbol{u} = \left(\frac{\partial}{\partial t} + U\frac{\partial}{\partial s}\right)^2 \boldsymbol{X}. \tag{3.10}$$

The force on the conduit per unit length due to the fluid, $\boldsymbol{F}$, is equal and opposite of the force on the fluid, which in turn is equal to the mass per unit length of the fluid times its acceleration as

$$\boldsymbol{F} = -\rho A \boldsymbol{a} = -\rho A \left(\frac{\partial}{\partial t} + U\frac{\partial}{\partial s}\right)^2 \boldsymbol{X} \tag{3.11}$$

Question 3.1. A section of a fluid carrying conduit has a square cross section of side b. In this section, the conduit curves along its length by a quarter circle with a radius of curvature R, which is much longer than b. The fluid has density ρ, and flows with an average speed U through the conduit. The conduit centerline is steady in time. Assuming the fluid to be inviscid and its velocity to be uniform across the conduit cross section, determine the net force it exerts on this section of conduit.

Answer 3.1. Left as an exercise to the reader. Note that the force may be determined in two ways: (i) Using a momentum balance on a control volume enclosing the fluid going through a quarter turn, (ii) By integrating the force determined using eq. (3.11). Both should yield the same expression for force.

Question 3.2. A flexible conduit shape oscillates sinusoidally such that its centreline follows the curve given by

$$\boldsymbol{X} = s\hat{\boldsymbol{e}}_x + a\Re(e^{i\omega t - iks})\hat{\boldsymbol{e}}_y, \tag{3.12}$$

where $a \ll 1$, k and ω are parameters. The conduit has a circular cross section with cross section area A uniformly along its length. The fluid inside is inviscid, has density ρ and speed U along the centreline. The fluid velocity profile may be assumed to be uniform across the cross section. Determine the force on such a conduit due to the fluid it carries.

Answer 3.2. Based on eq. (3.11), the force per unit length is

$$\boldsymbol{F} = \rho A a(\omega + kU)^2 \Re(e^{i\omega t - iks})\hat{\boldsymbol{e}}_y. \tag{3.13}$$

3.2.2 Thin layer flow

Consider a two-dimensional case with fluid sandwiched between two walls, as shown in fig. 3.2. The fluid has density ρ and viscosity μ. The bottom wall is flat and aligned with the x axis but the top wall, possibly made of some solid structure, is curved and unsteady as described by $y = h(x,t)$. The thickness of the fluid layer is small compared to its scale along the direction of the flow. The objective is to determine the fluid pressure so that the force on the wall at $y = h(x,t)$ may be determined.

Mass conservation

The fluid is incompressible, so the statement of mass conservation reduces to volume conservation. Using a control volume between x and $x + \mathrm{d}x$ yields the relation

$$\frac{\partial h}{\partial t} + \frac{\partial q}{\partial x} = 0, \quad \text{where} \quad q = \int_0^h u(x,y,t)\ \mathrm{d}y. \tag{3.14}$$

Here $q(x,t)$ is the flux of fluid volume across x.

When applying momentum balance, we must consider two extreme limits.

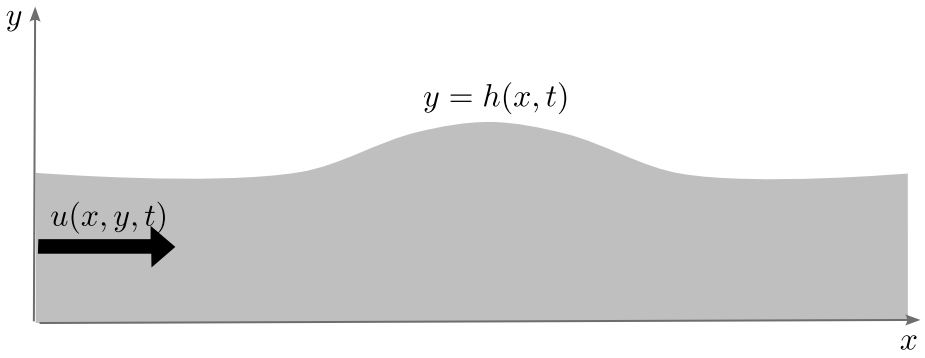

Figure 3.2: Fluid flow through a thin layer.

Momentum conservation – viscous case

In this case, inertia is negligible, and it is possible to show that by virtue of the thinness of the fluid layer, eq. (3.1) reduces to

$$\frac{\partial p}{\partial x} = \mu \frac{\partial^2 u}{\partial y^2}, \quad \Longrightarrow u = -\frac{1}{2\mu}\frac{\partial p}{\partial x}\, y(h-y). \tag{3.15}$$

In other words, the film is so thin that locally the flow quickly evolves into the Poiseuille parabolic profile we know and cherish. Here we have assumed a no-slip condition at $y = 0$ and $y = h$, but other boundary conditions may be accommodated without much difficulty. Integrating across the film thickness then yields the flux to be

$$q = -\frac{1}{12\mu} h^3 \frac{\partial p}{\partial x}. \tag{3.16}$$

Momentum conservation – inviscid case

If the fluid viscosity is to be neglected, the thickness-wise profile of the fluid velocity must be ascertained *ad hoc*. A common choice is to assume a top-hat or uniform profile of u across the thickness, so that the volume flux is

$$q = uh. \tag{3.17}$$

Momentum balance in this case invokes the inertia of the fluid in the form

$$\rho\left(\frac{\partial u}{\partial t} + u\frac{\partial u}{\partial x}\right) + \frac{\partial p}{\partial x} = f - d(u,h), \tag{3.18}$$

where f is the external force per unit volume acting on the fluid and $d(u,h)$ is the drag per unit volume exerted by the wall.

The momentum conservation closes the system and provides the fluid pressure in terms of the velocity and the motion of the wall.

Question 3.3. Onset of roll waves: A uniform thin film of fluid flowing under gravity rapidly down an incline of angle θ, when perturbed develops undulation in the free surface. Determine the criteria for the onset of such undulations. The wall drag may be taken to be in the form of a so-called Chezy friction

coefficient, C_f, as

$$d(u,h) = C_f \rho \frac{u^2}{h} \tag{3.19}$$

Answer 3.3. The question expects us to also develop a model for the flow. We suppose that the word "rapidly" implies a high Reynolds number, and hence are tempted to apply an inviscid thin film approximation. In this case, the top surface of the film is free so the pressure there is atmospheric (taken to be zero). As a result, the pressure at depth y is $p = \rho g(h-y)\cos\theta$ as determined by hydrostatic balance, since the velocity along y is negligible. Substituting this in the inviscid governing equations formed by eqs. (3.14), (3.17) and (3.18) then yields

$$\frac{\partial h}{\partial t} + \frac{\partial (uh)}{\partial x} = 0, \tag{3.20a}$$

$$\frac{\partial u}{\partial t} + u\frac{\partial u}{\partial x} + g\cos\theta \frac{\partial h}{\partial x} = g\sin\theta - C_f \frac{u^2}{h}. \tag{3.20b}$$

What follows is a linear stability analysis of a uniform steady state of these equations.

Note that a uniform steady state of these equations is $u = U$ and $h = H$ such that $g\sin\theta = C_f U^2/H$. Perturbing about this steady state as $u = U + u'$ and $h = H + h'$, where u' and h' are assumed to be infinitesimal, yield the following linear equations

$$\frac{\partial h'}{\partial t} + U\frac{\partial h'}{\partial x} + H\frac{\partial u'}{\partial x} = 0, \tag{3.21a}$$

$$\frac{\partial u'}{\partial t} + U\frac{\partial u'}{\partial x} + g\cos\theta \frac{\partial h'}{\partial x} = C_f \left(\frac{2U}{H} u' - \frac{U^2}{H^2} h' \right). \tag{3.21b}$$

It behooves us to examine perturbations of the form $(u', h') = (\hat{u}, \hat{h}) e^{st} e^{ikx}$, so that the eigenvalue equation for s in terms of k is in the form

$$s\hat{h} + ikU\hat{h} + ikH\hat{u} = 0, \tag{3.22a}$$

$$s\hat{u} + ikU\hat{u} + g\cos\theta ik\hat{h} = g\sin\theta \left(2\frac{\hat{u}}{U} - \frac{\hat{h}}{H} \right) \tag{3.22b}$$

Now we proceed with the following reasoning. We expect that as U increases, presumably because we are increasing the slope of the incline, at a critical value of U the perturbations will transition from exponential decay to exponential growth. At the transition, the perturbations neither grow nor decay. The complex nature of eq. (3.22) imply that the eigenvalue s must be purely imaginary at the threshold, i.e. say $s = -i\omega$ for some real ω. With this substitution, eq. (3.22a) implies that $(\omega - Uk)\hat{h} = Hk\hat{u}$, so that $\hat{u}$ and $\hat{h}$ may be taken to be purely real. Decomposing eq. (3.22b) into real and imaginary parts then yields $(\omega - Uk)\hat{u} = g\cos\theta k\hat{h}$ and $2H\hat{u} = U\hat{h}$. Eliminating ω, $\hat{u}$ and $\hat{h}$ then yields the threshold condition

$$\frac{U^2}{gH\cos\theta} = 2 \quad \text{or, equivalently,} \quad \tan\theta = 2C_f. \tag{3.23}$$

3.3 Conclusion

To study fluid-structure instabilities, it is necessary to understand and quantitatively represent the force transmitted between the fluid and the structure. It is frequently the case that the motion of the structure modifies the fluid flow, which then reacts by modifying the force exerted on the structure. The process of representing this relationship was considered in this chapter, especially in the form of simplified models. As always, the purpose of these models is to illuminate the underlying physical processes and facilitate insight.

Chapter 4

Galloping and flutter

Having laid the background needed in structures and fluids, we present in this chapter two fluid-structure instabilities – galloping and flutter. Both galloping and flutter arise as a consequence of the steady fluid dynamic characteristics of non-circular bodies. The civil engineering community encountered them in swaying of bridges in breezy conditions. The aerodynamics community experienced them in the flutter of wings. They are both considered to be part of the same family of fluid-structure instabilities. Galloping is considered to be behind the disastrous collapse of the Tacoma Narros bridge in 1940. These instabilities are far too common for design engineers to ignore them.

4.1 Galloping

Galloping is an instability brought about by the quasi-steady fluid dynamic characteristics of the body. This instability appears in many cases such as the oscillations of electric cables either by themselves or in response ice accumulation on them during cold winters. It also plagues civil structures such as bridges and towers. Generally, a single degree of freedom shows oscillations at or closer to the natural frequency of the structural mode, but a coupling between more than one degrees of freedom could also underlie the mechanism.

4.1.1 Translational galloping

The toy demonstrating the spontaneous oscillations of the cylinder with the D-shaped cross section supported on two springs is an excellent example of translational galloping. This toy was first presented as an example by Den Hartog[3] in 1956, a name which we will see again in this section. Figure 4.1 shows a schematic of this toy as a one-degree-of-freedom oscillator, consisting of a D-shaped mass m supported by a spring with stiffness k and a damper wth constant b. The flat face of the D-shaped cross section faces the oncoming wind with speed U, and, as a result, the the mass starts to oscillate. In the classroom demo, the D-shape has a diameter of about 5 cm, and oscillates with a frequency of about 2 Hz. Here we present the mechanism behind the spontaneous emergence of these oscillations in the form of an instability.

The state variable we invoke is the displacement of the mass perpendicular to the oncoming flow, which we denote $y(t)$. The state obeys

$$m\ddot{y} + b\dot{y} + ky = f, \tag{4.1}$$

where f is the aerodynamic force along y. Because of the symmetry of the D-shape, a steady state exists when $y = y_0 = 0$. In this case, f also vanishes. Therefore, we perturb this steady state as $y = y_0 + y'$, where y' is the perturbation. Now noting that the steady state is $y_0 = 0$, $y = y'$, so we might as well drop the prime on the y, a practice that is commonly followed and one that the author is eager to adopt. And eq. (4.1) is linear in y, so assuming y to be infinitesimal means we merely need to determine f when y is infinitesimal.

To determine the fluid dynamic force along y, we first test for quasi-steadiness. The structural natural frequency is $f \approx 2$ Hz, and the characteristic length scale for the flow to develop is the diameter D of the D-shape, and the flow speed is $U \approx 10$ m/s. So the reduced frequency is $fD/U \approx 0.01$. In other words, a fluid particle flows 100 diameter downstream by the time the structure completes one oscillation. This inspires us to treat the fluid dynamics as steady.

The y component of the force f derives contribution from two contributions, and both of them originate from examining the relative velocity of the fluid with respect to the body. Even an infinitesimal velocity of the mass changes the apparent orientation of the oncoming wind, even if it is by an infinitesimal amount, which we will now determine. The mathematical determination of this apparent wind is shown in fig. 4.1(b), where the

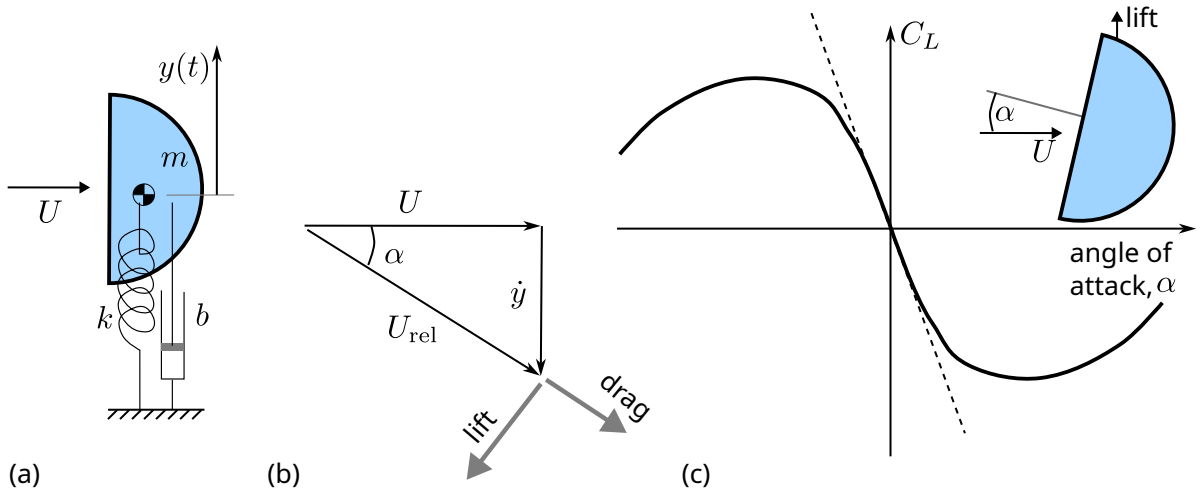

Figure 4.1: Translational galloping of a cylinder with a D-shaped cross section. (a) Schematic setup of the structural support for the cylinder and direction of oncoming wind. (b) The aerodynamic characteristics of the cross section.

mass is moving in the direction of positive y, which in the reference frame of the mass causes a component of flow in the negative y direction. The relative wind speed U_{rel} is given by

$$U_{\text{rel}} = \sqrt{U^2 + \dot{y}^2}, \tag{4.2}$$

and the apparent angle of attack α is given by

$$\alpha = \tan^{-1}\left(\frac{\dot{y}}{U}\right). \tag{4.3}$$

Only the linear terms in the approximations of U_{rel} and α need to be retained in eqs. (4.2) and (4.3), as required by linear stability analysis. This relative flow gives rise to a drag F_D and a lift F_L on the D-shaped cross section, which are aligned along the direction of relative speed and perpedicular to it, respectively. The lift and drag may be parameterized using lift and drag coefficients as

$$F_L = \frac{1}{2}\rho U_{\text{rel}}^2 A C_L(\alpha, \text{Re}), \qquad F_D = \frac{1}{2}\rho U_{\text{rel}}^2 A C_D(\alpha, \text{Re}), \tag{4.4}$$

where $\text{Re} = \rho U_{\text{rel}} D/\mu$ is the Reynolds number, ρ is the fluid density and μ its viscosity. The force f is then given by

$$f = -F_L \cos\alpha - F_D \sin\alpha. \tag{4.5}$$

We now approximate these quantities up to linear order in the perturbation y as

$$U_{\text{rel}} \approx U + \ldots, \tag{4.6a}$$

$$\alpha \approx \frac{\dot{y}}{U} + \ldots, \tag{4.6b}$$

$$F_L \approx \frac{1}{2}\rho U^2 A \left.\frac{\mathrm{d}C_L}{\mathrm{d}\alpha}\right|_{\alpha=0} \alpha + \ldots, \tag{4.6c}$$

$$F_D \approx \frac{1}{2}\rho U^2 A C_D|_{\alpha=0} + \ldots \tag{4.6d}$$

$$f \approx \frac{1}{2}\rho U A C_y \dot{y} + \ldots \tag{4.6e}$$

where

$$C_y = \left(-\left.\frac{\mathrm{d}C_L}{\mathrm{d}\alpha}\right|_{\alpha=0} - C_D|_{\alpha=0}\right). \tag{4.6f}$$

Here the two contributions behind the vertical fluid dynamic force f is as follows. Firstly, the drag is realigned in the direction of the apparent oncoming flow, which is now at an angle α and has a small component in the direction of motion proportional to the speed of the mass. This is the term proportional to C_D in eq. (4.6f). Secondly, the small angle of attack the D-shape makes to the oncoming flow gives rise to a proportional lift force. This lift is nearly in the direction of negative y, and gives rise to the term proportional to $\mathrm{d}C_L/\mathrm{d}y$ in eq. (4.6f). The resulting C_y is called the Den Hartog coefficient, which is a dimensionless expression of the fluid dynamic response.

We can now enter the phase of stability analysis. Replacing the aerodynamic force f from eq. (4.6e) in eq. (4.1), yields the coupled equation for the evolution of the fluid-structure state as

$$m\ddot{y} + b'\dot{y} + ky = 0, \tag{4.7}$$

where

$$b' = b + \frac{1}{2}\rho U A C_y \tag{4.8}$$

is the equivalent damping coefficient accounting for the aerodynamic force. The stability of the state $y = 0$ depends on the sign of the equivalent damping coefficient b'. We expect $C_D(\alpha = 0)$ to be positive for all shapes of the body, including the "D" shape cross section. For streamlined shapes, we expect C_L to be an increasing function of α, so that $\mathrm{d}C_L/\mathrm{d}\alpha$ is positive. However, for many bluff shapes, such as the D-shape, lift acts in the opposite direction. This is shown in fig. 4.1(c) The reader can imagine the reason based on how the stagnation pressure acting on the flat face forces the body. As a result, for many bluff cross sections, including the "D" shape and many common structural shapes such as the I and H beams, $\mathrm{d}C_L/\mathrm{d}\alpha$ is negative around $\alpha = 0$, and results in C_y being negative.

The usual stability calculation, which proceeds by expressing $y = \hat{y}e^{st}$, then determines exponential growth when b' is negative (see section 2.1, which also includes a non-dimensionalization). Based on this criterion, there exists a critical velocity U_{crit} given by

$$U_{\mathrm{crit}} = \frac{2b}{-\rho A C_y}. \tag{4.9}$$

For fluid velocity above this critical, galloping is spontaneously excited. This result is the culmination of the stability analysis.

4.1.2 Rotational galloping

Galloping instability may also appear in systems with one rotational degree of freedom, such as pitch, for bluff bodies. The treatment of fluid dynamics in this case is more empirical than for the translational case but follows along closely parallel lines The rotational degree of freedom is represented by the state variable θ, which obeys

$$I\ddot{\theta} + B\dot{\theta} + \kappa\theta = Q(\theta, \dot{\theta}), \tag{4.10}$$

where I is the moment of inertia of the object, B is the rotational damping coefficient, κ is the torsional spring constant, and Q is the fluid dynamic torque on the object. The rotational damping coefficient may be written in terms of a linear damping coefficient b as $B = bR_g^2$, just in the same way the rotational moment of inertia is written in terms of a mass $I = mR_g^2$, where R_g is the radius of gyration. It is also convenient to express $\kappa = kR_g^2$ for comparison with the translational galloping case. The argument then proceeds to justify that, in quasi-steady flow, the torque may be parameterized as

$$Q = \frac{1}{2}\rho U_{\mathrm{rel}}^2 A L_Q C_Q(\alpha, \mathrm{Re}), \tag{4.11}$$

where U_{rel} is the effective relative velocity, A is the frontal cross section of the object as before, L_Q is an additional length scale akin the distance between the centre of support and centre of pressure, and C_Q is the torque coefficient, which depends on an effective angle of attack, α. This effective angle of attack for a rotating body is then taken to be an average along the length of the body, and this is not quite rigorous. Yet, in the limit of infinitesimal perturbations, $\theta = \theta_0 + \theta'$, where θ_0 is a steady state, the torque parameterization reduces to

$$Q = \frac{1}{2}\rho U_{\mathrm{rel}}^2 A L_Q \frac{\mathrm{d}C_Q}{\mathrm{d}\alpha}\left(\theta' + \frac{L_\alpha}{U}\dot{\theta}'\right), \tag{4.12}$$

where L_α is another length scale that arises from the determination of the average angle of attack. (This part has no satisfactory justification but the forgiving reader can examine the dimensions for consistency. Loosely

speaking, $L_\alpha \dot{\theta}$ plays the same role that $\dot{y}$ played in the translational case in determining the effective angle of attack.) Substituting this torque in eq. (4.10) then yields a

$$m\ddot{\theta}' + b'\dot{\theta}' + k'\theta' = 0 \tag{4.13}$$

where

$$b' = \left(b - \frac{1}{2}\rho U A \frac{L_Q L_\alpha}{R_g^2} \frac{\mathrm{d}C_Q}{\mathrm{d}\alpha} \right) \tag{4.14}$$

$$k' = \left(k - \frac{1}{2}\rho U^2 A \frac{L_Q}{R_g^2} \frac{\mathrm{d}C_Q}{\mathrm{d}\alpha} \right). \tag{4.15}$$

At this stage the similarity between the translational and rotational cases of galloping is evident, except for one difference. In this case, the torsional spring is also modified, which can lead to the divergence instability we discussed in detail in chapter 1. Here we ignore that possibility and focus on galloping, which arises when b' becomes negative, which is possible if $\mathrm{d}C_Q/\mathrm{d}\alpha$ is positive. The critical velocity for rotational galloping is

$$U_{\text{crit}} = \frac{2b}{\rho A C_y} \quad \text{where} \quad C_y = \frac{L_Q L_\alpha}{R_g^2} \frac{\mathrm{d}C_Q}{\mathrm{d}\alpha}. \tag{4.16}$$

The astute reader will compare this critical velocity with the divergence speed to determine the mechanism to which a given structure is most susceptible.

4.1.3 Suppressing galloping

The advantage of the simple analysis presented in this section is that it provides us with insight into the physical mechanism of galloping instability, and in doing so provides us with methods of suppressing it. The critical velocity in eq. (4.9) directly embodies this insight. Firstly, note that in this case the excited frequency of oscillations is close to the natural frequency, slightly modified due to the damping coefficient. This follows directly from the analysis in section 2.1 applied to eq. (4.7). Secondly, the instability arises because the fluid dynamical characteristics, completely encapusilated in the Den Hartog coefficient C_y, overcome the internal structural damping b. The Den Hartog coefficient for various cross sections is presented in Table 4-1 (page 109) of book on Flow-induced Vibrations by Blevins[1]. This motivates the definition of a scale of velocity

$$U_{\text{gallop}} = \frac{2b}{\rho A}. \tag{4.17}$$

The magnitude of this velocity depends on the structural geometry (cross section area A, possibly ratio of lengths) and damping (coefficient b) relative to the fluid material characteristics (ρ). The criteria for spontaneous excitation may be written as $U_{\text{crit}} = U_{\text{gallop}}/|C_y|$, and offers the following interventions to suppress them. Galloping may be suppressed by increasing the structural damping. Doubling the damping coefficient doubles the U_{gallop}, and thus double the critical velocity. Galloping may also be suppressed by modifying the cross-section shape, for example, by streamlining it. This modifies C_y, and if the magnitude of C_y can be decreased, it increases the critical velocity. Note that stiffening the structure is expected to merely increase the natural frequency and have no influence on the galloping threshold.

4.2 Flutter

Flutter is the common term used to describe the oscillatory instability of a structure as described by aeronautical engineers. It was commonly observed as tips or control surfaces of aircraft wings and propeller blades exhibited violent vibrations usually due to the coupling and synchronization between two structural modes. Because of the myriad ways in which different modes of a structure could couple, understanding flutter was a historically challenging task, which lead one of the leading fluid dynamicist, Theodore von Karman, to claim[5], "Some fear flutter because they do not understand it, and some fear it because they do." An outline of the mechanism of flutter is presented below using the pitch-heave structure of chapter 2 in section 2.2.

Consider a streamlined lift-generating shape such as an airfoil in a flow supported by an elastic structure. The airfoil can pitch by angle θ and heave with displacement h, as shown in fig. 4.2, and thus h and θ for the state variables. The structural variables are identical to the ones defined in section 2.2, and in addition the airfoil is subject to a flow of a fluid of density ρ with speed U. The Reynolds number of the flow may be considered to be large, and the structural frequencies are slow relative to the fluid dynamic time scale so that the fluid dynamic response may be considered to be quasisteady.

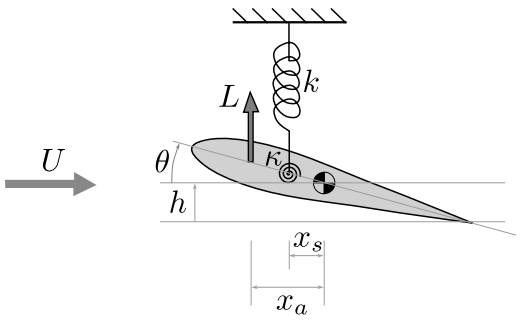

Figure 4.2: Schematic setup for flutter instability with pitch and heave degrees of freedom.

We neglect the aerodynamic drag in this situation because of the streamlined shape of the body. The lift on the body is given by

$$L = \frac{1}{2}\rho U^2 A C_L(\alpha, \mathrm{Re}) \tag{4.18}$$

where A is the area of the airfoil, C_L is the lift coefficient, α is the effective angle of attack and Re is the Reynolds number. The torque on the airfoil is written as Lx_a, where x_a is the distance of the centre of pressure from the centre of mass. We will drop the dependence of the lift coefficient on the Reynolds number, since it is usually quite weak.

The effective angle of attack arises from two effects, viz, the pitch of the airfoil, and its heave velocity. Similar to the analysis in section 4.1.1, especially eq. (4.3), the effective angle of attack is

$$\alpha = \theta - \tan^{-1}\left(\frac{\dot{h}}{U}\right). \tag{4.19}$$

We will limit our analysis to infinitesimal perturbations about $h = \theta = 0$ and in this case do not bother with the prime notation because $h = h'$ and $\theta = \theta'$. In this case,

$$\alpha \approx \theta - \frac{\dot{h}}{U}. \tag{4.20}$$

Based on this, the equations governing the evolution of the state are

$$m\ddot{h} + kh + kx_s\theta = \frac{1}{2}\rho U^2 A \frac{\mathrm{d}C_L}{\mathrm{d}\alpha}\left(\theta - \frac{\dot{h}}{U}\right), \tag{4.21a}$$

$$I\ddot{\theta} + kx_s h + \kappa\theta = \frac{1}{2}\rho U^2 A x_a \frac{\mathrm{d}C_L}{\mathrm{d}\alpha}\left(\theta - \frac{\dot{h}}{U}\right). \tag{4.21b}$$

Now is a good moment to take stock of the parameters and their dimensions.

Question 4.1. Non-dimensionalize eq. (4.21) and determine the dimensionless parameters that govern the dynamics.

Answer 4.1. We employ the same non-dimensionalization for the structural variables as in eq. (2.21),

$$t = \tilde{t}T, \quad h' = R_g\tilde{h}, \quad \theta' = \tilde{\theta}, \tag{4.22}$$

where $T = \sqrt{\dfrac{m}{k}}$, which results in two dimensionless structural variables

$$\delta = \frac{2x_s}{R_g}, \quad \text{and} \quad \omega_a^2 = \frac{\kappa}{kR_g^2}, \tag{4.23}$$

and three dimensionless fluid dynamic variables

$$\varphi = \frac{1}{2}\frac{\rho U^2 A}{kR_g}\frac{\mathrm{d}C_L}{\mathrm{d}\alpha}, \quad \tau = \frac{R_g}{UT}, \quad \text{and} \quad \delta_a = \frac{2x_a}{R_g}. \tag{4.24}$$

The dimensionless equations for $\tilde{h}$ and $\tilde{\theta}$ are

$$\frac{\mathrm{d}^2\tilde{h}}{\mathrm{d}\tilde{t}^2} + \tilde{h} + \frac{\delta}{2}\tilde{\theta} = \varphi\left(\tilde{\theta} - \tau\frac{\mathrm{d}\tilde{h}}{\mathrm{d}\tilde{t}}\right), \tag{4.25a}$$

$$\frac{\mathrm{d}^2\tilde{\theta}}{\mathrm{d}\tilde{t}^2} + \frac{\delta}{2}\tilde{h} + \omega_a^2\tilde{\theta} = \varphi\frac{\delta_a}{2}\left(\tilde{\theta} - \tau\frac{\mathrm{d}\tilde{h}}{\mathrm{d}\tilde{t}}\right). \tag{4.25b}$$

Here φ is the dimensionless fluid velocity, τ is the ratio of fluid dynamic time scale to the structural one, and δ_a measures the offset of the centre of pressure.

As question 4.1 shows, there are five dimensionless parameters. Of these five, we have already recognized that τ is small. This is the parameter that measures the strength of the structural timescale to the fluid dynamic time scale, and we have determined that the structure moves much slower compared to how fast the fluid reacts. Hence we justifiably neglect the terms proportional to τ. If an instability is to materialize, we anticipate φ to be the critical parameter.

We now proceed to determining the modes and their exponential growth or decay. Substituting $(\tilde{h}, \tilde{\theta}) = (\hat{h}, \hat{\theta})e^{i\omega\tilde{t}}$ gives the eigenvalue equation for the frequency ω as

$$\omega^2\begin{bmatrix}\hat{h}\\ \hat{\theta}\end{bmatrix} = \begin{bmatrix}1 & \delta/2 - \varphi\\ \delta/2 & \omega_a^2 - \varphi\delta_a/2\end{bmatrix}\begin{bmatrix}\hat{h}\\ \hat{\theta}\end{bmatrix} \tag{4.26}$$

and the characteristic equation

$$\begin{aligned}&(\omega^2 - 1)\left(\omega^2 - \omega_a^2 + \varphi\frac{\delta_a}{2}\right) - \frac{\delta}{2}\left(\frac{\delta}{2} - \varphi\right)\\ &= \omega^4 - \omega^2\left(1 + \omega_a^2 - \varphi\frac{\delta_a}{2}\right) + \omega_a^2 - \frac{\delta^2}{4} + \varphi\left(\frac{\delta - \delta_a}{2}\right) = 0.\end{aligned} \tag{4.27}$$

Of course, it is possible to solve this quadratic in ω^2 to get an analytical expression for the frequency, but we seek insight more than an analytical expression. So we proceed as follows.

First, note that when $\varphi = 0$, the characteristic equation reduces to eq. (2.25). Therefore, the sum and difference of squared frequencies of the purely structural modes is $\omega_1^2 + \omega_2^2 = 1 + \omega_a^2$ and $\Delta\omega^2 \equiv \omega_1^2 - \omega_2^2 = \sqrt{\delta^2/4 + (1 - \omega_a^2)^2}$. Second, note that since the coefficients of the quadratic in eq. (4.27) are all real. Hence the only possibilities are:

1. Both roots of the quadratic are positive real numbers. In this case, the four values of ω are purely real appearing in pairs as $\pm\omega_1$ and $\pm\omega_2$ because both roots are positive. There is no instability in this case.
2. One of the roots of the quadratic, say ω_2^2, becomes negative. In this case, there are two imaginary root $\pm\omega_2$, and one of them causes the perturbation to grow exponentially in time.
3. The quadratic has complex roots, in which case, two of the four roots for ω will cause exponential growth of the perturbation.

The case where one of the roots of the quadratic becomes negative is easier to analyze. The threshold criterion is that one root of the quadratic is zero, which leads to the condition

$$\varphi = \frac{\omega_a^2 - \dfrac{\delta^2}{4}}{\frac{1}{2}(\delta_a - \delta)}. \tag{4.28}$$

Question 4.2. Re-dimensionalize equation eq. (4.28) to find an equation for critical value of U and discuss the physics behind the threshold.

Answer 4.2. The equivalent dimensional expression for U is

$$U = \sqrt{\frac{2\kappa'}{\rho A(x_a - x_s)(\mathrm{d}C_L/\mathrm{d}\alpha)}}. \tag{4.29}$$

Here we have used the definition $\kappa = \kappa' + kx_s^2$. This expression is similar to eq. (1.20), and in fact generalizes the criteria for divergence for arbitrary locations of centre of mass, centre of support and centre of pressure. Note that the centre of mass does not enter this result. Only the torsional spring constant enters the expression for the critical velocity, thus implying that this mechanism engages only the pitch degree of freedom. This expression also shed further insight into the mechanism for divergence. It necessarily occurs when the centre of pressure is upstream of the centre of support.

The reason divergence appears as an instability in this analysis is because all the ingredients needed for divergence are present in this system, and therefore, the threshold for divergence must arise as a possibility from the analysis. This result is that possibility.

Based on the analysis in question 4.2, we can eliminate divergence from our analysis and now focus on the third possibility for an instability: complex roots of the quadratic. This occurs when the discriminant of the quadratic becomes negative.

Question 4.3. Determine the criteria on δ, δ_a and ω_a^2 that there exists a value φ where the discriminant of the quadratic in eq. (4.27) is negative.

Answer 4.3. This condition is

$$\left(1 + \omega_a^2 - \varphi\frac{\delta_a}{2}\right)^2 - 4\left[\omega_a^2 - \frac{\delta^2}{4} + \varphi\left(\frac{\delta - \delta_a}{2}\right)\right] \leq 0, \tag{4.30}$$

$$\text{or equivalently, } \left(1 - \omega_a^2\right)^2 + \delta^2 - \varphi\delta_a(1 + \omega_a^2) + \varphi^2\frac{\delta_a^2}{4} + 2\varphi(\delta_a - \delta) \leq 0. \tag{4.31}$$

This condition looks satisfactory on its face, and at the same time produces little physical insight. To further illuminate the physics, let us recognize the appearance of $\Delta\omega^2$, and determine the value of φ which leads to the smallest value for the discriminant. Noting that the smallest value of the quadratic $a\varphi^2 - 2b\varphi$ is $-b^2/a$ and applying it to eq. (4.31) gives

$$(\Delta\omega^2)^2 \leq \frac{\left[(1 + \omega_a^2)\delta_a + 2(\delta - \delta_a)\right]^2}{\delta_a^2}. \tag{4.32}$$

Exploiting the squares on both sides, and using the following properties that necessarily hold true:

1. $\omega_a^2 \geq 1$ because $\kappa = \kappa' + kx_s^2$,
2. $1 + \omega_a^2 = \omega_1^2 + \omega_2^2$ and $\Delta\omega^2 = \omega_1^2 - \omega_2^2$, where $\omega_{1,2}$ are defined in eq. (2.25),

then yields the following condition for the discriminant to be negative

$$\frac{\delta}{1 - \omega_1^2} \leq \delta_a \leq \frac{\delta}{1 - \omega_2^2}. \tag{4.33}$$

The diligent reader will find it irresistible to write eq. (4.33) in its dimensional form and realize that it constraints the location for the centre of pressure, which makes the structure susceptible to flutter. The structure is susceptible to this flutter instability even when the centre of pressure is behind the centre of support. This result reveals the frustrating aspect of aeroelastic instabilities that when the divergence instability is eliminated, the system becomes susceptible to flutter.

The mechanism of flutter is as follows. The structure has two independent modes of oscillation in the absence of the fluid. These modes couple the heave and the pitch degrees of freedom. The fluid flow further modifies these modes, and when the conditions are just right, bring the modal frequencies closer together. The strength of the flow needed to brings these frequencies together depends on the separation between them. The closer they are, the weaker the flow needed to induce flutter. Once they coincide, a coherence between the pitch and the heave are established. The mode that amplifies the motion is the one which synchronizes the lift with the heave velocity. This requires the pitch angle have a component in phase with the heave velocity. This requirement is

seen most conveniently in the energy equation, which can be derived in dimensionless form from eq. (2.23) as

$$\frac{1}{2}\frac{\mathrm{d}}{\mathrm{d}\tilde{t}}\left[\left(\frac{\mathrm{d}\tilde{h}}{\mathrm{d}\tilde{t}}\right)^2+\left(\frac{\mathrm{d}\tilde{\theta}}{\mathrm{d}t}\right)^2+\tilde{h}^2+\left(\omega_a^2+\phi\frac{\delta_a}{2}\right)\tilde{\theta}^2+\delta\tilde{h}\tilde{\theta}\right]=\phi\frac{\mathrm{d}\tilde{h}}{\mathrm{d}\tilde{t}}\tilde{\theta}. \tag{4.34}$$

Thus, energy is pumped into the coupled mode if and only if θ has some component in phase with $\dot{h}$. This synchronization cannot happen without the frequencies of the two modes matching, and thus the threshold is essentially set by the frequency matching condition.

4.2.1 Suppressing flutter

Unlike galloping, increasing damping or adding it if it does not exist is not the most effective method to suppress flutter. It is so because the core mechanism of flutter relies on structural synchronization, and therefore the best intervention is one that disrupts it. Common approaches include stiffening the torsional defree of freedom so that its natural frequency is well separated from the bending or heave degree of freedom. Doing so is not only effective but also economical.

4.3 Conclusion

Divergence, galloping and flutter are some of the basic fluid-structure instabilities, which inflict a large number of engineering systems from civil, mechanical to aeronautical ones. In all these cases the mode excited is a slightly modified version of the structural modes. On the time scale of these modes, the fluid adjusts rapidly to the instantaneous configuration of the structure. These forces then inject energy into the structural modes and cause their amplitude to grow.

Chapter 5

Vortex induced vibrations

The instability of galloping and flutter excite the natural mode of vibration of the structure in a situation where the fluid dynamic time scale is well-separated from the motion of the structure. The two scales are not so separated in the case of vortex induced vibrations. Underlying the vortex-induced vibrations is the purely fluid-dynamical instability of vortex shedding.

Any cylindrical bluff body immersed in a steady uniform flow sheds vortices alternating between each side of the body. Successive vortices are shed from alternating sides, even if the body cross section shape is symmetric. The vortex shedding has a well-defined frequency when the body is held stationary. These vortices are carried downstream and form the well-known von Karman vortex street. This phenomenon of vortex shedding is quite generic and is observed from the milimeter to the geological scales. For example, the vortex shedding past an island in the Pacific ocean is shown in fig. 5.1.

This causes a lift force of alternating sign on the body, which in turn causes the body to oscillate. The oscillations are naturally pronounced when the natural frequency of the structure that supports the body matches the naturally frequency of vortex shedding. Remarkably, if the natural structural frequency differs from the natural vortex shedding frequency, the process of vortex shedding alters itself so that vortices are shed at the natural frequency of the structure. These features of the phenomenon are the topic of this chapter.

5.1 Fluid dynamical instability

Consider a two-dimensional cross section shape, which is symmetric about the x-axis, with a characteristic length D. As an example, we will use the circular cross section with diameter D. This shape is subject to a uniform flow of speed U. The fluid is incompressible, has viscosity μ and density ρ.

The state variable is the Eulerian velocity field $\boldsymbol{u}(\boldsymbol{x}, t)$, which obeys the incompressible Navier-Stokes equations

$$\rho\left(\frac{\partial \boldsymbol{u}}{\partial t} + (\boldsymbol{u}\cdot\boldsymbol{\nabla})\boldsymbol{u}\right) = -\boldsymbol{\nabla}p + \mu\nabla^2\boldsymbol{u}, \quad \text{and} \quad \boldsymbol{\nabla}\cdot\boldsymbol{u} = 0. \tag{5.1}$$

The variables are non-dimensionalized as presented in section 3.1 resultin in the dimensionless equations eq. (3.2)

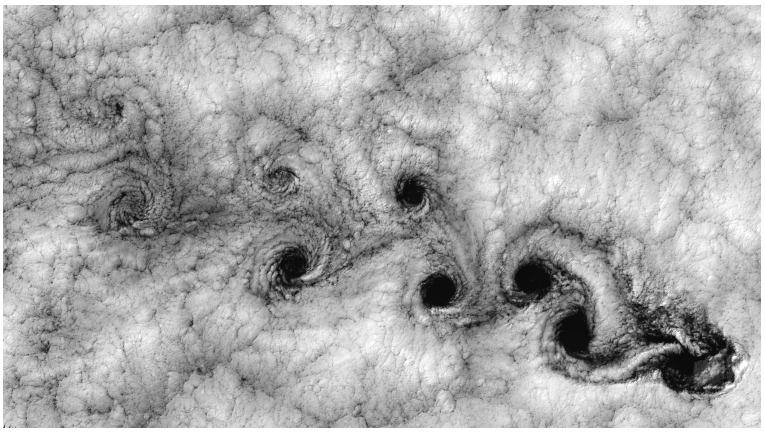

Figure 5.1: von Karman vortex street generated as wind flows past the Juan Fernandez island, which is visualized in satellite imagery by passing clouds.

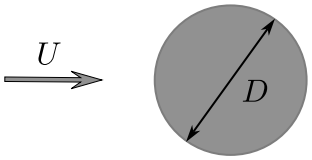

Figure 5.2: Schematic of the setup for analyzing vortex shedding.

reproduced here as

$$\frac{\partial \boldsymbol{u}}{\partial t} + (\boldsymbol{u}\cdot\boldsymbol{\nabla})\boldsymbol{u} = -\boldsymbol{\nabla} p + \frac{1}{\mathrm{Re}}\nabla^2\boldsymbol{u}, \quad \text{and} \quad \boldsymbol{\nabla}\cdot\boldsymbol{u} = 0, \tag{5.2}$$

where we have dropped the tilde decoration on the dimensionless variables for convenience, and chosen $L = D$ for the length scale and $T = D/U$ for the time scale. These are partial differential equations for the components $\boldsymbol{u} = (u, v)$, which must be supplemented with appropriate boundary conditions. These are

$$\boldsymbol{u} = \boldsymbol{0}, \quad \text{on the surface of the circle,} \tag{5.3a}$$
$$\boldsymbol{u} = \hat{\boldsymbol{e}}_x, \quad \text{as } |\boldsymbol{x}| \to \infty. \tag{5.3b}$$

Since no analytical solution to these equations with these boundary conditions is known, we must now proceed computationally. The solutions presented here are found using the commercial software COMSOL.

Here are the steps in the linear stability analysis. For each Reynolds number in a range, the steady state $\boldsymbol{u} = \boldsymbol{u}_0(\boldsymbol{x}; \mathrm{Re})$ is first calculated. An example is shown in fig. 5.3. The state is then perturbed as $\boldsymbol{u} = \boldsymbol{u}_0 + \boldsymbol{u}'$, and the governing equations for $\boldsymbol{u}'$ linearized as

$$\frac{\partial \boldsymbol{u}'}{\partial t} + (\boldsymbol{u}_0\cdot\boldsymbol{\nabla})\boldsymbol{u}' + (\boldsymbol{u}'\cdot\boldsymbol{\nabla})\boldsymbol{u}_0 = -\boldsymbol{\nabla} p' + \frac{1}{\mathrm{Re}}\nabla^2\boldsymbol{u}', \quad \text{and} \quad \boldsymbol{\nabla}\cdot\boldsymbol{u}' = 0, \tag{5.4}$$

where p' is the corresponding perturbation in pressure. Here we have used our judgment to non-dimensionalize the variables earlier in the process, so that step is not necessary any more. Hence we proceed to the next step of determining the eigenvalue problem by substituting $\boldsymbol{u}' = \hat{\boldsymbol{u}}e^{st}$, so that the mode shape $\hat{\boldsymbol{u}}$ and growth rate s satisfies

$$s\hat{\boldsymbol{u}} + (\boldsymbol{u}_0\cdot\boldsymbol{\nabla})\hat{\boldsymbol{u}} + (\hat{\boldsymbol{u}}\cdot\boldsymbol{\nabla})\boldsymbol{u}_0 = -\boldsymbol{\nabla}\hat{p} + \frac{1}{\mathrm{Re}}\nabla^2\hat{\boldsymbol{u}}, \quad \text{and} \quad \boldsymbol{\nabla}\cdot\hat{\boldsymbol{u}} = 0, \tag{5.5}$$

where $\hat{p} = p'e^{-st}$ is the variable corresponding to pressure. There is a distinct possibility that the instability is oscillatory, so $\hat{\boldsymbol{u}}$, $\hat{p}$ and s are taken to be complex numbers.

The solution of the eigenvalue problem in eq. (5.5) is outside the scope of this document. (A sample will be shared in class from Zebib (1987)[10].)

All eigenvalues have a negative real part for $\mathrm{Re} < \mathrm{Re}_c \approx 47$, where Re_c is the critical Reynolds number. When the Reynolds number equals the critical value, the real part of two eigenvalues vanishe, while that of all the others remain negative. When the Reynolds number exceeds the critical, the real parts of those two eigenvalues are positive and signals exponential growth of the corresponding mode shape. Here two modes simultaneously become unstable because eigenvalues and eigenvectors must appear in complex conjugate pairs, so that the real perturbation that grows may be written as

$$\boldsymbol{u}' = c_1\hat{\boldsymbol{u}}e^{st} + c_1^*\hat{\boldsymbol{u}}^*e^{s^*t}, \tag{5.6}$$

where superscript $*$ denotes complex conjugation.

The imaginary part of the eigenvalue, $\omega = \Im(s)$, then gives the frequency of oscillations of the flow perturbation, which grows. This is, therefore, related to the (dimensional) frequency, f, of vortex shedding of the growing perturbation as $f = \omega U/2\pi D$. The frequency of vortex shedding is usually represented by the Strouhal number, $\mathrm{St} = fD/U$, which is then related to ω as $\mathrm{St} = \omega/2\pi$. Just as Re_c is independent of the size of the cylinder or the nature of the fluid, St also represents the shedding frequency in a scale-independent manner. According to linear stability analysis, the St at the critical Re is around 0.1. However, the dynamics changes as the perturbation grows and reaches a finite amplitude, when it starts growing. In that state, the vortex shedding frequency is characterized by $\mathrm{St} \approx 0.2$. Experimentally measured Strouhal numbers as a function of Reynolds number for different shapes from page 50 of the book by Blevins[1] is shared separately in a handout.

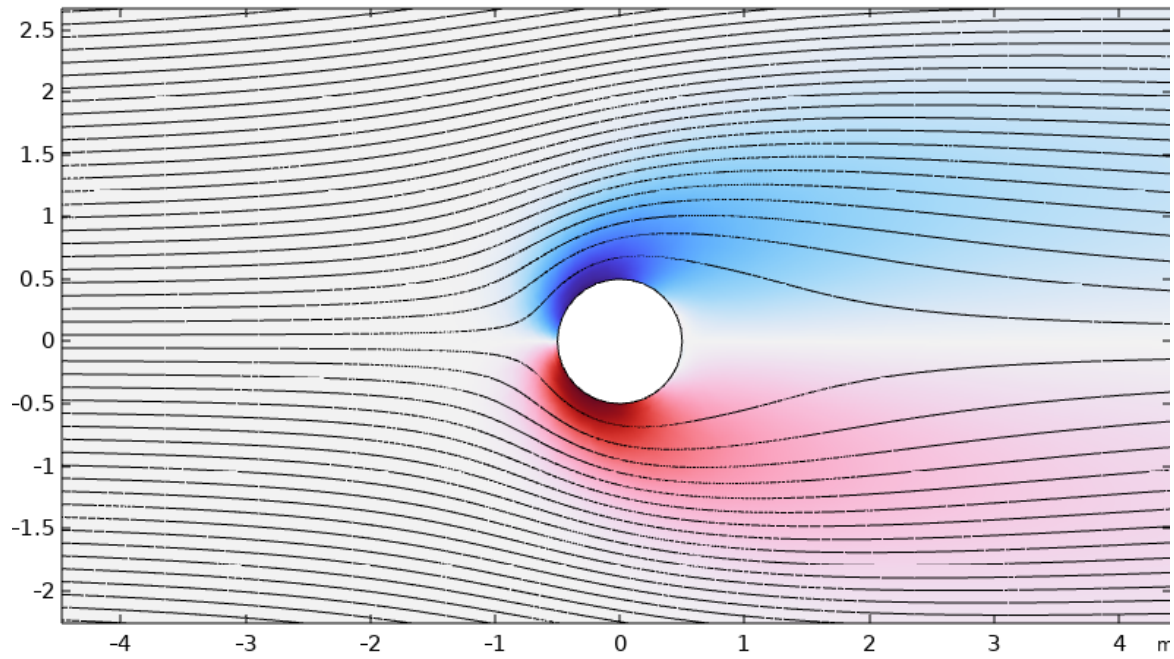

Figure 5.3: Steady state of eqs. (5.2) and (5.3) at Re = 10. Colours (shown in the document online) denote vorticity (red is positive and blue is negative). Black lines show streamlines.

The last piece of the puzzle is lift force on the cylinder. This is now an oscillating quantity with the same frequency as the vortex shedding and an amplitude that in a dimensionless form potentially depends on the Reynolds number and the object shape. This dependence is expressed as the lift coefficient as a function of Reynolds number, for example on page 64 of Blevins[1].

So far we have summarized the nature of the fluid dynamical instability that underlies vortex shedding around stationary cylinders. If the cylinders are mobile, we can now attempt to describe their response.

5.2 Vortex-induced vibrations

The basic idea is to model the cylinder as a one-dimensional structure with a mass, spring and damper, which is forced at the vortex shedding frequency in the direction of lift. If the displacement of the cylinder is y, then following the notation of eq. (2.1), y satisfies

$$m\ddot{y} + b\dot{y} + ky = F_L \sin \omega t, \tag{5.7}$$

where F_L is the amplitude of the lift force and ω is the (dimensional) frequency.

Question 5.1. Determine the steady periodic $y(t)$ satisfying eq. (5.7) and the amplitude of $y(t)$.

Answer 5.1. We start with non-dimensionalization, identical to that presented in eqs. (2.1) and (2.3), to get

$$\ddot{y} + 2\beta\dot{y} + y = \sin \Omega t, \tag{5.8}$$

where we have dropped the tilde decoration and defined the non-dimensionalization of y in terms of F_L/k, and $\Omega = \omega/\omega_0$. (The reader is reminded that y was not non-dimensionalized in eq. (2.3).)

The solution is

$$y(t) = a \sin(\Omega t - \phi), \quad \text{where} \quad a = \left[(1-\Omega^2)^2 + (2\beta\Omega)^2\right] \quad \text{and} \quad \tan\phi = \frac{2\beta\Omega}{1-\Omega^2}. \tag{5.9}$$

Re-dimensionalizing the solution in eq. (5.9) is now a routine matter to predict the vortex-induced vibrations. This task is left to the industrious reader.

5.3 Mode locking

Due to this is a remarkable feature of vortex-induced vibrations, called mode locking, the structure can modify the vortex shedding frequency to a small extent. Suppose the (dimensional) natural frequency of the structure is ω_0 and the natural vortex shedding frequency is ω_f, which are close to each other. Then the fluid dynamical vortex shedding instability is altered by the possible motion of the structure so that the joint vortex-induced vibrations frequency is ω_0.

5.4 Response to vortex shed by identical neighbours

Special care must be taken when designing identical structures that are susceptible to vortex-induced vibrations near each other, especially when no mechanism for damping is included. This is so because vortices shed that are shed from one structure apply an oscillating force on the second structure,so if the second is exactly downstream of the first when vortex-induced vibrations commence, the second become vulnerable to an additional forcing from the vortices of the first.

The following question illustrates this point.

Question 5.2. Two poles 20 m tall and 0.2 m in diameter are erected 30 cm apart. Each pole is cantilevered to ground and free at the top. The pole is essentially a 1 cm thick pipe made of steel (density 7850 kg/m^3 and Young's modulus 200 GPa). Wind blows in a direction such that the wake of first pole is incident on the second, causing an oscillating lift force on the second. The second pole itself sheds vortices. The combined effect of the two processes is that the net amplitude of the oscillating lift on the second pole may be taken to be $C_L = 1.3$.

1. Determine the natural frequency of the fundamental mode of oscillations of the tower.
2. Let us take the Strouhal number for vortex shedding to be 0.2. Determine the wind speed for which the shedding frequency matches with the structural frequency of the fundamental mode.
3. Assume the wind speed is according to the value found in the previous part. The drag coefficient for a cylinder is 0.7. Calculate the steady deflection of the pole. Ignore variation of the drag along the length of the pole.
4. Assuming that the pole could still be considered to be straight, write the equation for the amplitude, $a(t)$, of the fundamental mode of oscillation forced by the alternating lift force. Again, assume that the lift does not vary with length.
5. Solve this equation and determine the amplitude of the tip of the pole.

Answer 5.2. We answer in parts.

1. Based on the geometry, the second moment of the cross section, I is

$$I = \pi(R_o^4 - R_i^4) = 1.08 \times 10^{-4} \text{ m}^4,$$

where R_o and R_i are the outer and inner radii of the tower. Based on this, the bending rigidity of the tower $B = EI$ is

$$B = EI = 2.16 \times 10^7 \text{ N m}^2,$$

where E is the Youngs modulus. Using the density of steel, ρ, the mass per unit length, μ of the tower is

$$\mu = \rho\pi(R_o^2 - R_i^2) = 46.9 \text{ kg/m}.$$

Hence, from eq. (2.56), the natural frequency Ω_1 of the fundamental mode is

$$\Omega_1 = k_1^2\sqrt{\frac{B}{\mu L^4}} = 37 \text{ rad/s}, \quad f_1 = \frac{\Omega_1}{2\pi} = 6 \text{ Hz},$$

where f_1 is the freuqncy.

2. Using the definition of the Strouhal number and its value of 0.2

$$U = \frac{f_1 D}{\mathrm{St}} = 6 \text{ m/s} \approx 20 \text{ km/h}.$$

3. Let ρ_a be the density of air. The steady force on the pole per unit length is

$$f_D = \frac{1}{2}\rho_a U^2 (2R_o) C_D = 3 \text{ N/m}.$$

The tip deflection, δ, is

$$\delta = \frac{f_D L^4}{8B} = 2.7 \text{ mm}.$$

4. The deflection of the beam satisfies

$$\mu \frac{\partial^2 h}{\partial t^2} + B\frac{\partial^4 h}{\partial x^4} = -\frac{1}{2}\rho_a U (2R_o) C_D \frac{\partial h}{\partial t} + \frac{1}{2}\rho_a U^2 (2R_o) C_L \sin \Omega_1 t.$$

In this equation, the term proportional to C_D is determined from considerations identical to eq. (4.6). A moments inspection will immediately convince the reader that the term proportional to C_D act as a damping and is relatively quite weak compared to either the inertial term or the bending term for the fundamental mode of vibrations. Yet it is important to retain this term. Multiplying by the mode shape, $y_1(x/L)$ from eq. (2.57), and integrating gives the equation for the amplitude of fundamental mode as

$$\ddot{a} + 2\beta\dot{a} + \Omega_1^2 a = f_L \sin \Omega_1 t,$$

where

$$f_L = \frac{1}{2}\frac{\rho_a U^2 (2R_o) C_L}{\mu}\left(\frac{\int_0^1 y_1(s)\ \mathrm{d}s}{\int_0^1 y_1^2(s)\ \mathrm{d}s}\right) \approx 0.10 \text{ m/s}^2 \quad \text{and} \quad \beta = \frac{1}{4}\frac{\rho_a U (2R_o) C_D}{\mu} \approx 5.3 \times 10^{-3} \text{ s}^{-1}.$$

Here, the mode shape is scaled such that $y_1(1) = 1$, so that the deflection of the tip is unity.

5. The solution proceeds along the lines similar to question 5.1 but is simplified because the forcing frequency is equal to the natural frequency. In this case the solution is

$$a(t) = -a_0 \cos \Omega_1 t \quad \text{where} \quad a_0 = \frac{f_L}{2\beta\Omega_1} \approx 25.7 \text{ cm!}$$

The amplitude of the vortex-induced vibrations is nearly a 100 times bigger than the static deflection of the pole under the wrong wind conditions.

Note that in question 5.2, the dominant damping of the vibrations comes from the fluid itself. The metal itself provides extremely small amount of damping, which is why tuning forks vibrate for as long as they do. Radiation of sound from the vibrations is another source of damping, the dominant one for the tuning fork, but for the pole sound radiation is negligible compared to the damping due to the drag.

Finally, note that for a single pole, vortex-shedding applies a lift force with $C_L \approx 0.2$, so that the deflection of the upstream pole would be smaller by a factor $1.3/0.2 \approx 6.5$. But it is the vortices shed by the upstream pole that causes and much larger oscillating force on the downstream one. If these structures are designed merely to sustain their own vortex shedding force, without accounting for the vortices shed from the other pole, they would almost certainly fail when the wind aligns.

5.5 Suppressing vortex-induced vibrations

Mechanisms to suppress vortex-induced vibrations fall in the following categories:

1. Avoiding resonance by stiffening the structure. This intervention is obvious to avoid large amplitude oscillations.

2. Streamline the cross section. Doing so reduces the possibility of alternate vortices shed and also reduces their strength by diminishing their magnitude. It may not always be possible to change the cross section.

3. Add vortex suppression device. These devices disrupt the synchrony of the vortex-shedding process. Examples include helical strakes, perforated shrouds, axial slats, etc. These examples and more are shown in Figure 3-23 on page 78 of the book by Blevins[1].

4. Add or increase damping. This method is not always possible or may be too expensive. Dampers may be passive, such as a dashpot, or active, such as the tuned-mass damper. An entertaining account is presented in this popular video.

5.6 Conclusion

Vortex-induced vibrations are an example of a flow instability that drives a structure. This is unlike the other examples we have seen, such as galloping and flutter. In all these example, the natural modes of oscillation are excited by a fluid flow, whether or not the flow adjusts quasisteadily to the instantaneous geometry of the structure. We have presented the outline of the purely fluid dynamical instability in section 5.1 and then the forcing of the structural mode in section 5.2. However, this treatment is approximate because the in the fluid dynamical stability analysis, the no-slip boundary condition was imposed on the surface of the stationary cylinder. In vortex-induced vibrations, the cylinder is not stationary. Thus, our analysis is necessarily approximate. The exact linear stability analysis with the moving cylinder is outside the scope of this document.

Chapter 6

Conduits and channels

Flow through enclosed spaces could interact with the surrounding material and spontaneously cause motion to arise through an instability. Much of life depends on fluid flow interacting with elastic solids gives rise to spontaneous oscillations. The phonation in our vocal cords is a prime example of a steady flow exciting an oscillation, which is radiated as sound. The reader can imagine many other sounds generated by similar mechanisms. The topic is vast and the objective of this chapter is to provide the reader with an appreciation of this topic.

6.1 An infinite firehose

Tubes and pipes carrying fluid often deform away from their straight shape when the flow rate through them exceeds a critical value. Straight pipes can spontaneously curve or start oscillating because the straight shape is unstable. In cases, such as the whipping of a firehose, the instability is driven by the reaction force on the hose as the fluid leaves it. Such a force can easily be calculated using control volume analysis, such as the kind you learned in IB. The possibility is not merely academic, but is a serious engineering concern, as these videos and numerous others on the internet demonstrate (see video 1, video 2).

The hose is also unstable to perturbation away from an exit. To understand the principles behind this instability, consider an infinite conduit under tension T carrying an inviscid fluid of density ρ at speed U, as shown in fig. 6.1. The cross section of the conduit is uniform along its length with area A, and the conduit has mass μ per unit length. The unperturbed shape of the conduit is straight, say along the x direction, and the fluid flows parallel to the local centreline of the conduit. The fluid dynamics is identical to the setup described in section 3.2.1, whereas the structural dynamics derives from section 2.4.

The steady centerline of the conduit is $\boldsymbol{X}(s,t) = s\hat{\boldsymbol{e}}_x$ and let us perturb it perpendicular to its length as$\boldsymbol{X}(s,t) = s\hat{\boldsymbol{e}}_x + y(s,t)\hat{\boldsymbol{e}}_y$, where $y(s,t)$ is an infinitesimal transverse displacement. The equation governing the perturbation is

$$\mu\frac{\partial^2 y}{\partial t^2} = T\frac{\partial^2 y}{\partial s^2} - \rho A\left(\frac{\partial}{\partial t} + U\frac{\partial}{\partial s}\right)^2 y. \tag{6.1}$$

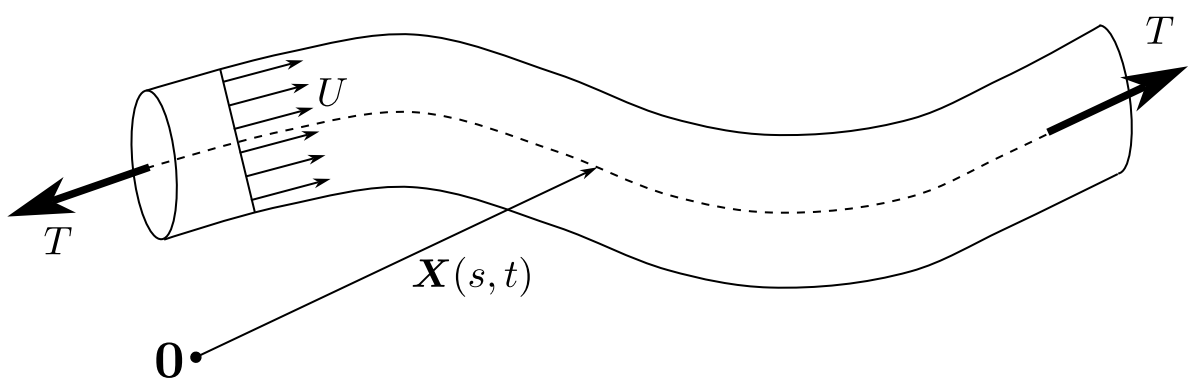

Figure 6.1: Schematic of the infinite-conduit, reproduced from fig. 3.1.

(Note that we have circumvented the details of the steps writing the equation governing a finite perturbation and then linearizing it for small magnitude. Also, we have dispensed with the prime notation for perturbations.)

We now seek modes in the form $y(s,t) = \hat{y}(s)e^{i\omega t}$, where $\hat{y}$ satisfies

$$-\mu\omega^2\hat{y} = T\frac{\mathrm{d}^2\hat{y}}{\mathrm{d}s^2} - \rho A\left(i\omega + U\frac{\mathrm{d}}{\mathrm{d}s}\right)^2\hat{y} \quad \Longrightarrow \quad (T-\rho AU^2)\frac{\mathrm{d}^2\hat{y}}{\mathrm{d}s^2} - 2i\omega\rho AU\frac{\mathrm{d}\hat{y}}{\mathrm{d}s} + \omega^2(\mu+\rho A)\hat{y} = 0, \tag{6.2}$$

This is a constant coefficient ordinary differential equation, in an infinite domain $-\infty < s < \infty$. The solution to this equation is clearly of the form e^{rs} for some r, but the perturbation can neither grow as s approaches either ∞ or $-\infty$. Therefore, the only possibility is that r is purely imaginary, and the solution oscillates. It is customary to take $r = ik$, where k is called the wavenumber (of course, the symbol k is of no consequence, and cam be replaced by another convenient symbol). This observation turns eq. (6.2) into the dispersion relation

$$\omega^2(\mu+\rho A) + 2\rho UA\omega k - (T-\rho AU^2)k^2 = 0. \tag{6.3}$$

Observe that in the absence of the fluid ($\rho = 0$) the dispersion relation reduces to that of a stretched string, $\omega = \pm k\sqrt{T/\mu}$. In the presence of the fluid but in the absence of the flow ($\rho \neq 0$ but $U = 0$), the mass per unit length increases to $\mu + \rho A$. In both these cases, ω is purely real, implying that any perturbation travels as a wave which neither grows not decays. Since eq. (6.3) is a quadratic for ω with real coefficients, and the solutions are real when $U = 0$, the solutions are bound to remain real for small values of U. Instability is possible only if ω has a negative imaginary part, i.e. when ω is complex. Complex roots for ω are possible when U exceeds a threshold, which can be determined by setting the discriminant to negative as

$$(\rho AU)^2 + (\mu+\rho)(T-\rho AU^2) < 0. \tag{6.4}$$

Solving for the U yields the threshold

$$U > \sqrt{\frac{T}{\mu^*}} \quad \text{where} \quad \frac{1}{\mu^*} = \frac{1}{\mu} + \frac{1}{\rho A}. \tag{6.5}$$

At the critical U, the quadratic has two identical roots equal to

$$\omega = -\frac{kU}{\mu/\mu^*}, \tag{6.6}$$

which defines the speed of the growing perturbation, $\omega/k = U(\mu^*/\mu)$ at the threshold.

The physics of this instability is as follows. The fluid dynamical force on the conduit arises from the curvature of the streamlines, which arises from the curvature of the centreline. This curvature creates a pressure difference across the conduit, which exerts an unbalanced force on the conduit in a direction that increases the curvature (i.e. centrifugal). The magnitude of this force is proportional to ρU^2, and it gets stronger with faster flow. When it exceeds the restoring force of tension, the perturbation spontaneously grows.

Question 6.1. Non-dimensionalize eq. (6.1) and repeat the linear stability analysis in dimensionless terms. How many dimensionless numbers exist in this formulation?

Answer 6.1. The answer is left as an exercise for the reader to practice the art of dimensional analysis.

6.2 An infinite channel with flexible walls

Inspired by the general model of a flow in a narrow space, such as through the vocal folds, consider the flow through a thin channel bounded by a stretched membrane, as shown in fig. 6.2. The elastic membrane is a model for a more general elastic structure. The membrane has mass μ per unit area and tension per unit length T, so its shape $h(x,t)$ satisfies

$$\mu\frac{\partial^2 h}{\partial t^2} = T\frac{\partial^2 h}{\partial x^2} + p(x,t), \tag{6.7a}$$

where p is the fluid pressure in the fluid pressure in the channel. The fluid in the channel has density ρ and a fluid velocity $u(x,t)$ that is uniform across the channel height and width. The fluid conservation equations

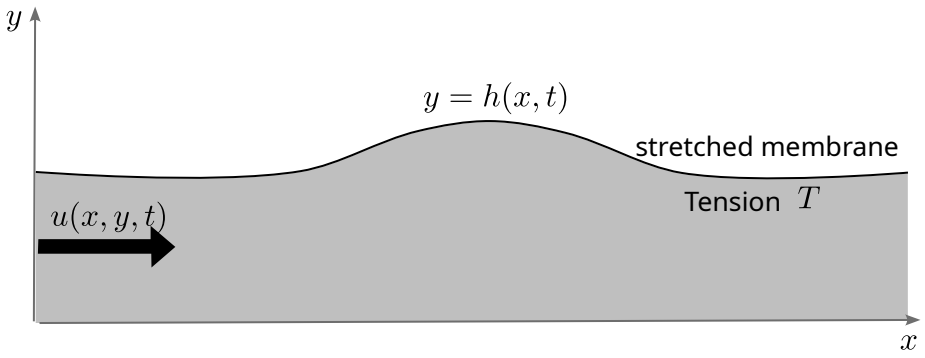

Figure 6.2: Schematic of flow through a thin channel with a bounding flexible membrane.

satisfy

$$\frac{\partial h}{\partial t} + \frac{\partial (uh)}{\partial x} = 0, \tag{6.7b}$$

$$\rho \left(\frac{\partial u}{\partial t} + u \frac{\partial u}{\partial x} \right) + \frac{\partial p}{\partial x} = 0. \tag{6.7c}$$

Equations (6.7b) and (6.7c) resemble eqs. (3.14) and (3.18), respectively, with $f = d(u, h) = 0$. The purpose of this analysis is to examine the role of inertia of the fluid with the inertia and the elasticity of the surrounding structure. (A separate analysis can be carried out where the role of friction is examined in the absence of inertia.) Hence, as a deliberate choice with the intention of eliminating all extraneous physical effects, we accept f and $d[u, h]$ to be zero.

Question 6.2. Assume that the channel is infinite in length. Then the state $u(x, t) = U$, $p(x, t) = 0$, and $h(x, t) = H$, where U and H are constants, is a steady state of eq. (6.7). Perform a linear stability analysis for a perturbation with wavenumber k and determine the threshold velocity U in terms of the other parameters for small perturbations to grow.

Answer 6.2. The threshold is

$$U_{\text{critical}} > \sqrt{\frac{T}{\mu^*}}, \quad \text{where} \quad \frac{1}{\mu^*} = \frac{1}{\mu} + \frac{k^2 H}{\rho}. \tag{6.8}$$

Filling in the details constitutes an excellent exercise for the indefatigable reader.

Let us now interpret the result in question 6.2. Just as eq. (6.5) in section 6.1, μ^* is an effective mass per unit area, which combines the inertia of the membrane and the fluid in the channel. This μ^* depends on the wavenumber k, i.e. on the wavelength of the perturbation, and through it the threshold velocity U_{critical} also depends on k. Of all the possible wavenumbers (i.e. wavelength), $k = 0$ gives the lowest threshold $U_{\text{critical}} = \sqrt{T/\mu}$. Thus, we conclude that the uniform state $u = U$, $h = H$ will be impossible to maintain if U exceeds the wave speed on the membrane $\sqrt{T/\mu}$. Based on this result, we suspect that for a finite channel and membrane, we expect the longest mode that fits in the domain to determine the threshold velocity. Of course, for a finite channel, boundary conditions will also play a role in determining the fate of any perturbation.

6.3 Conclusion

These are just two of the numerous examples possible of instability that arises when a structure interacts with a flowing fluid. The reader will benefit immensely in gaining a deeper understanding of the topic if they can formulate a modification of one of the problems in this document. For example, how could the singing of telephone wires hanging in the wind be described? Or the wild oscillations of iced electric cables in wind?

How would the results of this chapter be modified in the firehose had a bending rigidity instead of being under tension? And for that matter, how could the oscillations of the vocal folds as we speak be described? Musical instruments, especially woodwinds, also have such instabilities underlyng their sound production mechanism. We leave the reader with these thoughts to ponder and with best wishes.

Bibliography

[1] Robert D Blevins. Flow-induced vibration. *New York*, 1977.

[2] Subrahmanyan Chandrasekhar. *Hydrodynamic and hydromagnetic stability*. Courier Corporation, 2013.

[3] Jacob Pieter Den Hartog. *Mechanical vibrations*. Courier Corporation, 1985.

[4] Philip G Drazin and William Hill Reid. *Hydrodynamic stability*. Cambridge university press, 2004.

[5] Isadore E Garrick and Wilmer H Reed III. Historical development of aircraft flutter. *Journal of Aircraft*, 18(11):897–912, 1981.

[6] John Happel and Howard Brenner. *Low Reynolds number hydrodynamics: with special applications to particulate media*. Springer Science & Business Media, 2012.

[7] Vivek Mukhopadhyay. Historical perspective on analysis and control of aeroelastic responses. *Journal of Guidance, Control, and Dynamics*, 26(5):673–684, 2003.

[8] G. I. Taylor. Film notes for Low Reynolds number flows, 1967. web.mit.edu/hml/ncfmf/07LRNF.pdf.

[9] G. I. Taylor. Low Reynolds number flows and reversibility, 1967. www.youtube.com/watch?v=rA6T83FKuE8. (For the full film see: /www.youtube.com/watch?v=51-6QCJTAjU).

[10] A Zebib. Stability of viscous flow past a circular cylinder. *Journal of Engineering Mathematics*, 21(2):155–165, 1987.